AD-A244 055

ION PAGE

Form Approved
OMB No 0704-0188

September 1991	3 REPORT TYPE AND DATES COVERED: Final Report 4/89 - 4/91

4 TITLE AND SUBTITLE

Studies of Gas Turbine Heat Transfer:
Airfoil Surfaces and End-Wall Cooling Effects

5. FUNDING NUMBERS

61102 F
2307
D S

(2)

6 AUTHOR

E.R.G. Eckert, R. J. Goldstein, S. V. Patankar and
T. W. Simon

AFOSR-TR- 91 0954

7 PERFORMING ORGANIZATION NAME AND ADDRESS

Heat Transfer Laboratory
Department of Mechanical Engineering
University of Minnesota
111 Church St. S.E.
Minneapolis, MN 55455

8 PERFORMING ORGANIZATION REPORT NUMBER

F49620-89-C-0060

9 SPONSORING MONITORING AGENCY NAME AND ADDRESS

Air Force Office of Scientific Research
Bolling Air Force Base, D.C.

10 SPONSORING MONITORING AGENCY REPORT NUMBER

F49620-89-C-0060

91-19212

DTIC
ELECTE
DEC 30 1991
S D
D

12a DISTRIBUTION CODE

Unclassified/Unlimited

Original contains color plates: All DTIC reproductions will be in black and white

The report documents accomplishments made toward understanding the fluid flow and heat transfer processes in gas turbines at the University of Minnesota over the past two years. The research is divided into three subtopics: studies of film cooling, airfoil surface heat transfer and endwall flow and heat transfer. Film cooling experiments show the effects of interaction among jets on curved surfaces and calculations show that parabolic techniques give accurate effectiveness predictions in regions away from injection holes. The surface heat transfer program showed that tripping the flow or roughening the wall has a clear effect near airfoil transition and separation points and that recovery from concave curvature is surprisingly slow. Endwall studies show flow visualization on the cascade endwall and the value of a fence on the endwall for rerouting the horseshoe vortex away from the suction wall.

14 SUBJECT TERMS	15. NUMBER OF PAGES
Gas Turbines, Film Cooling, Heat Transfer, Turbulence, Endwalls	42
	16. PRICE CODE

17 SECURITY CLASSIFICATION OF REPORT	18 SECURITY CLASSIFICATION OF THIS PAGE	19 SECURITY CLASSIFICATION OF ABSTRACT	20 LIMITATION OF ABSTRACT
u	u	u	unlimited

91 12 27 084

Final Report

to

The Air Force Office of Scientific Research

Studies of Gas Turbine Heat Transfer: Airfoil Surfaces and End-Wall Cooling Effects

AFOSR Grant No. F49620-89-C-0060
15 April 1989 - 30 April 1991

E.R.G. Eckert, R.J. Goldstein, S.V. Patankar and T.W. Simon
Co-Principal Investigators

September 1991

FOREWORD

The following report documents accomplishments made toward understanding the fluid flow and heat transfer processes in gas turbines. It covers the period of contract number F49620-89-C-0060 which has now come to a close. Papers which present major findings from the Heat Transfer Laboratory on gas turbine heat transfer are listed in Appendix I. This list is restricted to papers published, during and later than, 1988. Progress reports, proposals and abstracts which have given the details of work in progress, for their respective periods, are listed in Appendix II. This submittal emphasizes the accomplishments since the most recent progress report submitted in June, 1990.

The research is divided into three subtopics: film cooling studies, airfoil surface heat transfer studies, and endwall flow and heat transfer.

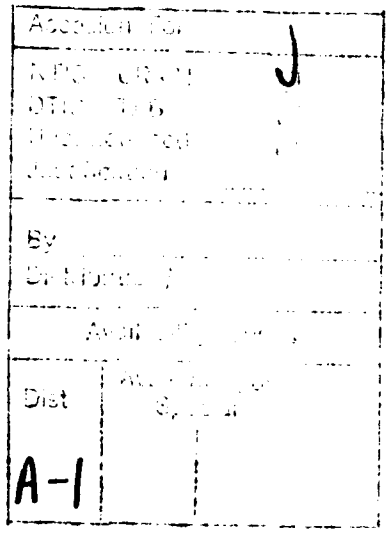

TABLE OF CONTENTS

I. FILM COOLING STUDIES

A. Interpretation of Effectiveness

A study investigated our present ability to predict the thermal performance of film cooling arrangements used to protect the hot components of gas turbines. The required information is usually obtained by model experiments carried out at near room temperature as opposed to the high temperature encountered in the gas turbines. Dimensional or similarity analysis is used to develop the functional relationships between film effectiveness and convective heat transfer. The use of mass transfer experiments with foreign gas injection and naphthalene sublimation based on the heat-mass transfer analogy is discussed. The law of superposition is used to describe the combined effects of film cooling, surface convection or radiation and frictional heating. An order of magnitude estimate indicates to what extent local temperature gradients are alleviated in the cooled walls by internal heat conduction.

B. Experiments

Effectiveness measurements and flow visualization of injection through a row-of-holes on curved surfaces were completed. The range of parameters include density ratios of one and two, blowing rates from 0.25 to 2.50, injection angles of 15, 25, and 45 degrees to the mainstream, and wall curvatures $2r/D = \pm 90$.

In terms of laterally-averaged effectiveness the injection angle is found to be of secondary significance compared to three dominating, independent variables: wall curvature, density ratio, and blowing rate. If these three, dominating variables are specified, the laterally-averaged film cooling effectiveness can be found to within ± 0.05 over most of the data set, from graphs such as Figure 1 a-f.

Lateral profiles of effectiveness, however, are strong functions of injection angle and blowing rate. Perhaps the most interesting finding of this experiment is that, although low injection angles yield somewhat higher film cooling effectiveness values at moderate blowing rates (since the resulting jet trajectories are closer to the wall), at high blowing rates the steeper jets can yield higher laterally-averaged effectiveness values. The nature of this role reversal is related to differences in lateral spreading rates, hence interactions among the jets, and the resulting occurrence of coolant touchdown between the jets for steep injection and high blowing rates. Thus, a short distance downstream of injection, under such conditions, effectiveness is low along the centerline of injection, due to lift-off, but high midway between the holes where coolant touches down (Fig. 2). These results are being prepared for publication.

C. Computation

Injection of cold secondary fluid into a hot mainstream results in a complex flow and heat transfer problem. The discrete hole cooling configuration is a common method employed in modern gas turbines and combustion chambers to shield metal surfaces from hot gases. The effectiveness of such systems is governed by a number of geometric and flow parameters viz. angle of injection, blowing rates, spacings between the holes, and the characteristics of the mainstream and injected jet turbulence. Experimental evidence also indicates the influence of pressure gradient and curvature of the wall on the cooling performance. Developing methods to predict the performance of the various cooling configurations has been the goal of several researchers for more than a decade.

The three dimensional computational procedure developed by Patankar and Spalding (1972) was used by Patankar et al. (1973) to predict the slot film cooling effectiveness. Bergeles et al. (1976, 1978) used the partially parabolic three dimensional procedure of Pratap and Spalding (1976) to predict the performance of discrete hole cooling situations. In the present report, the results of computations performed using the fully-parabolic approach are presented. The aim of the current research is to establish the zone of applicability of the computationally efficient fully-parabolic solution procedure in predicting the flow and heat transfer in the injection cooling systems. Comparisons with the available experimental data and with the results of partially-parabolic and locally-elliptic methods are reported. The present report is also concerned with the situation where the injected jets are directed lateral to the mainstream flow. A significant aspect of this problem is the periodic boundary condition prescription at the lateral boundaries of the computational domain. This allows the fluxes to leave and enter the domain from the lateral edges. The flow is assumed to be parabolic in the mainstream direction. The turbulent transport quantities are calculated with the two-equation, k-ε turbulence model.

1) The Physical and Computational Problem

The injection cooling situations considered in this paper are shown in Fig. 3 consisting of hot gases flowing over an adiabatic flat plate with a free-stream velocity of W_{in}. The injection is achieved through a row of holes of diameter D and spaced by a distance of s. The injected jet is directed at an angle β to the plate and its value is varied in the course of the investigation. The effect of blowing rate, M, on the cooling performance is studied using different velocities of the injected, jet V_{inj}. The density ratio of the jet fluid to the main-stream fluid is kept constant at unity throughout this study. Owing to the symmetry of the flow and the heat transfer for the streamwise injection case, the

computational domain in the x direction is shown by the region between the dotted lines in Fig. 3a. The domain extends to ten hole-diameters in the y direction. The inlet plane for this three-dimensional problem is placed 20 hole-diameters upstream of the injection holes and since a marching procedure is used to analyze the problem, the outflow plane downstream of the hole is not prescribed. Injection though a single hole is also investigated in this paper. As the spacing between the holes s is increased, a single hole configuration is obtained as a limiting case of a row of holes geometry. A spacing between the holes of 10 hole-diameters provided a computational domain significantly free of interactions between the neighboring jets across the planes of symmetry.

In the lateral injection, the jets are inclined at angles β to the plate and ϕ to the main stream. Figure 3b shows the details of the problem along with the essential geometric parameters. When the lateral angle $\phi = 0$ the streamwise injection problem is obtained while a purely lateral injection situation results when $\phi = 90^{o}$. In the present paper the injection angle β is kept constant at 30^{o}, while the lateral angle, ϕ, is given three values of $0, 45^{o}$, and 90^{o}. In addition the spacing between the holes, s, and the blowing rate, M, are varied. Because of periodicity in the x-direction, the computational domain is restricted to the region between the dotted lines shown in Fig. 3b. The top boundary is extended to 5 hole-diameters in the y-direction. The placement of the upper boundary at 10 and 15 hole-diameters did not alter the results in the region of interest. The cross-sectional plane is discretized into rectangular control volumes in a Cartesian grid. The control-volume sizes are chosen to be nonuniform with finer control volumes near the wall boundary at $y = 0$ and around the hole location in the x direction. The elliptic cross-section of the injection hole is approximated by rectangular control-volumes in the x-z plane. The forward steps Δz in the marching direction are also nonuniform; particularly small steps are used at stations around the injection holes.

2) Governing Equations and Turbulence Model

The governing equations for steady, three-dimensional turbulent flow in terms of the time-averaged quantities are equations of conservation of mass, momentum and energy. The Reynolds stress terms in the momentum equations are expressed in terms of turbulent viscosity μ_t (in the conventional isotropic model) and gradients of mean velocities. Bergeles, Gosman and Launder (1978) proposed an anisotropic modification to the stress terms, which increased the cross-stream diffusion based on an experimental correlation from Quark and Quarmby. According to this model if μ_{tx} and μ_{ty} are the diffusivities in the x and y directions then the two diffusivities are related by

$$\frac{\mu_{tx}}{\mu_{ty}} = 1 + \alpha$$

where, $\alpha = 3.5\,(1 - y/\Delta)$ if $y < \Delta$,

$\alpha = 0$ if $y > \Delta$

with Δ denoting the local boundary layer thickness and μ_{ty} is assumed to be equal to the isotropic eddy viscosity estimated by the turbulence closure model used. The anisotropic diffusion model is extended to the scalar energy transport in a manner similar to the momentum transport. Therefore, the ratio of the x direction turbulent diffusivity to the y direction turbulent diffusivity is $1+\alpha$, where α is defined as in the momentum equations.

The k-ε turbulence model

The standard k-ε model developed by Launder and Spalding (1974) is used to formulate an expression for the turbulent viscosity. The model involves the transport equations for the turbulent kinetic energy k and the rate of dissipation ε. The empirical constants of the regular k-ε model are used. The turbulent viscosity is much greater than the molecular viscosity for most of the flow, but near the wall the two viscosities are comparable. The wall functions (Launder and Spalding, 1974) are used to deduce the effective diffusivities in the near-wall region. The k-ε turbulence model has been successfully tested for many problems in two dimensions and a few three dimensional cases.

The transport equations for the momentum, energy and turbulence quantities are elliptic in nature. In this analysis, however, the flow is assumed parabolic in the mainstream direction (z-direction), hence the streamwise diffusion is neglected and the reverse flow precluded. In addition, the mainstream velocity is assumed to be governed by a cross-sectionally uniform average pressure gradient.

Boundary and Inlet Conditions

The boundary conditions need to be specified at the four boundaries of the cross-sectional plane and at the inlet plane. The top boundary is treated as a no-flux boundary. At the bottom wall, the wall function approach is adopted and the thermal condition on the wall is adiabatic.

The inlet boundary is placed ten diameters upstream of the hole-plane and uniform w-velocity W_{in}, k and ε are prescribed. Uniform profiles are also assumed for velocities at the jet exits. The thermal boundary condition at the inlet is that of uniform temperature T_∞ and the temperature of the coolant jet at the injection hole is T_c. The boundary conditions for k and ε at the injection hole are evaluated from the injection velocity .

In the streamwise injection case, symmetry conditions are employed at x/D = 0 and x/D = 1.5 by setting the normal velocity, U, and the normal gradients of all other variables equal to zero. The lateral boundaries of the lateral injection case, on the other hand, must account for the fluxes leaving and entering the domain in the lateral direction. These boundaries are treated as periodic boundaries; the details of this treatment are discussed in the next section.

In the parabolic procedure, the outflow plane and the conditions on it need not be prescribed. The computations are simply terminated at the desired z/D location.

3) The Calculation Procedure

The Three Dimensional Parabolic Procedure

The equations governing the transport of mass and momentum are a set of nonlinear coupled partial differential equations. The differential equations are integrated over the control volumes to give a set of algebraic discretization equations. The power-law scheme of Patankar (1980) is used for the formulation of the combined convection-diffusion fluxes. The details of the algebraic equations are discussed by Patankar (1980) for a general elliptic problem and by Patankar and Spalding (1972) and Pratap and Spalding (1976) for the parabolic-type problems.

A marching scheme is employed in which the momentum, continuity, turbulence and energy equations are solved on each plane starting from the inlet. The overall procedure remains the same as presented by Patankar and Spalding (1972); and therefore will not be described in detail here. Only the salient features will be mentioned. The cross-stream velocity-pressure coupling is treated by the SIMPLER algorithm of Patankar (1980). The streamwise pressure gradient, assumed constant for each cross section in the solution of the streamwise momentum equation, is obtained from the integral mass conservation as suggested by Raithby and Schneider (1979). The discretized energy equation is solved only once at each cross-stream plane after a converged solution for the flow equations is obtained. The converged solution of the previous step is used as the initial guess for the iterative solution of the current step.

The algebraic set of equations for each variable is solved in a segregated manner and a Tri-Diagonal Matrix Algorithm (TDMA) is employed as the basic solver. A block-correction procedure, in which uniform corrections are applied for strips in the x and y directions, is used to enhance the convergence of the TDMA procedure; details of the procedure are given by Settari and Aziz (1973).

The discretization of the domain, in which the governing equations are solved, is done in the x-y plane using rectangular grids. The cross-sectional plane is discretized into a

22 x 22 grid for the single hole geometry and 17 x 22 for the row of holes geometry for the streamwise injection case whereas 22 x 22 grid was used for the lateral injection problem. The grid structure, in both the cases, is non-uniform especially in the y-direction where finer grids are used near the wall. The marching step Δz is also non-uniform with smaller values in the region around the hole. A typical number of forward steps in this study is 100, though in certain cases different numbers have been used to obtain data at an experiment conforming z/D location.

Exploratory runs were also made with 32 x 32 and 44 x 44 grids in the x - y plane. Doubling the number of grids resulted in less than 2% difference in the values of temperatures and streamwise velocities at corresponding locations in the post-injection region. The typical CPU time for the cases evaluated in this work is approximately 9.5s for a 22x22x75 grid on the CRAY-2. The maximum difference in the values of temperature and streamwise velocity at the same z/D location was found to be less than 2 % for a 40x40 grid compared with a 22x22 grid in the cross-sectional plane.

Implementation of the Periodic Boundary Condition

The incorporation of the periodic nature of the lateral boundaries is done at the level of formulating the discretization equations. If the grid points are numbered 1, 2, 3, ... N, then the periodic boundary implies that, for grid point 1, the neighboring points in a computational sense are 2 and N. Similarly, for grid point N, the neighboring points are (N-1) and 1. The solution of such a cyclic system of equations is discussed in detail by Patankar et al. (1977) and is called the Cyclic-TDMA procedure. A block-corrected form of the CTDMA is applied to enhance the convergence.

4) Results and Discussion

Numerous cases were studied in the course of this work, most of them matching the conditions under which the experiments were performed. Since, the number and the detail are too many, a comprehensive summary of the cases is not included, instead the details are quoted along with the relevant figures.

Many comparisons of effectiveness, local and laterally averaged, with experiments and other numerical approaches are discussed in this section. Firstly, we discuss the performance of the method for the single hole geometry and subsequently the results of injection through a single row of holes with streamwise injection and lateral injection are presented.

Single Hole Streamwise Injection

The results in this subsection are compared with those of Bergeles et al. (1978). Figures 4a - 4d show the variation of the effectiveness, at four lateral locations, with the non-dimensionalized z-direction. Figures 4a and 4b show the present predictions for the blowing rates of 0.1 and 0.2 to agree with the experiments as well as the numerical predictions, in Fig. 4b, of a partially-parabolic approach. When the blowing rate is increased to 0.3, in Fig. 4c, a discrepancy in the prediction of effectiveness is observed in the experimental and numerical results. However, this discrepancy is confined to about eight diameters downstream of the injection port and the results are in good agreement with the experiments further downstream. This suggests that the local ellipticity in pressure (and velocity) does not significantly affect the performance of the solution procedure in the regions away from the injection hole. This point is further confirmed in the Fig. 4d where a similar trend is observed for a high blowing rate of M = 1.0. It is noticeable that the partially-parabolic procedure is also incapable of handling the elliptic characteristic of the velocity at high blowing rates, but the far field (beyond 10 diameters) results show a reasonable agreement.

Single Row of Holes Streamwise Injection

Figures 5a and 5b compare the results, obtained for the injection through a row of holes separated by a distance of s/D = 3 and at an angle of 35^{o} to the plate, with the experimental data of Kadotani (1975). The numerical predictions are in good agreement with the experimental findings for both the blowing rates of M = 0.5 and M = 0.2 considered. It is noteworthy that the anisotropic turbulence augmentation is successful in estimating the lateral cooling performance, showing reasonable agreement at the midplane between the holes (x/D = 1.5) with the experimental results. This enhanced performance can be seen in a greater detail in Fig. 6, where the results of the present computation are compared with the experimental data due to Kadotani and Goldstein (1977) and the numerical predictions using the locally-elliptic procedure by Demuren and Rodi (1983). The numerical predictions are not in good agreement with the experiments at z/D = 6.65 downstream of the injection port, but the agreement improves further downstream, as seen at a distance of z/D = 15.8 and 37.37. This result is analogous to the observations in the single hole study, but the noticeable feature is the competitive performance of the fully-parabolic procedure with the locally-elliptic procedure.

Single Row of Holes Lateral Injection

The computed result for the blowing rate of M = 0.5 and spacing of s/D = 5 is compared with the measurements of Honami and Fukagawa (1987). The experiment study included the measurements of lateral injection ($\phi = 90$) over a flat surface and is the basis of this comparison. The matching with the experiment is done to the extent of the available information viz. inlet velocity, injection hole diameter, the temperature difference between the mainstream and the secondary stream, turbulence intensity. Figure 7 shows a good agreement in the lateral distribution of cooling effectiveness at two location downstream of the injection hole. The fully-parabolic model is thus found to be adequate for this blowing rate. The effect of blowing rate on the distribution of the local effectiveness is also observed in Fig. 7 for M values of 0.1, 0.2, 0.5, and 1.0. The increased interaction between the jets and the improved cooling performance at higher blowing rates is the subject of the subsequent discussion. Since there is a lack of extensive experimental data for the lateral injection, we use this comparison and the experience of the authors with the model as the basis for the following analysis.

The motivation to study the lateral injection is to study the interaction of the injected jets with each otner and its effect on the full coverage cooling. The parametric study of the effects of the blowing rate, spacing between the holes and the lateral angles of injection is reported by Sathyamurthy and Patankar (1990). When the blowing rate is increased in the case of lateral injection, the cooling effectiveness tends to increase monotonically. On the other hand, the trend for the streamwise injection ($\phi = 0$) is that the cooling increases up to a blowing rate of 0.5 and then decreases. This is clearly seen in Fig. 8. The implication of this finding is that the lateral cooling configuration does not suffer from the blowing rate ceiling. The reason for such a behavior is that in the streamwise injection, there is a pair of counter-rotating vortices whose strength is proportional to the blowing rate. This causes the injected jet to be lifted off the surface at higher blowing rates and penetrate the boundary layer. As a result, the cold jet mixes with the hot mainstream and the cooling performance suffers. The lifting of the injected jet also allows the hot mainstream to flow under the jet thus decreasing the effectiveness. The lateral injection, on the other hand, generates a single dominant vortex structure (per hole) downstream of the injection. In spite of the increase in the strength of the secondary flow (vortex) with blowing rate, the secondary flow has larger tendency to push the jet in the lateral direction. Thus, the jet remains closer to the surface and leads to its higher cooling potential. Figure 9 shows the two different secondary flows resulting from the injections in the streamwise and lateral directions. Figure 10 shows the effect of the blowing rate on the local cooling of the surface and the higher blowing rate of M = 1 is seen to have a better coverage than the lower blowing rates.

5) Concluding Remarks

Numerical results of the film cooling by injection from a row of holes and a single hole are presented. Comparisons with the experiments and other numerical investigations demonstrate that the fully parabolic procedure is competitive in the quality of prediction compared with both the partially-parabolic and the locally-elliptic methods, while superior in terms of computing time and resources required. The computed results are in good agreement with the measurements of Honami and Fukagawa (1987) for the case of lateral injection. Furthermore, the following may be concluded from the present investigation:

a) The cases with angular injections and medium blowing rates are not dominated by strong elliptic effects (both pressure and velocity).

b) The elliptic effects in the higher end of medium blowing rate spectrum (around M = 1.0) are localized to a small region aft of the hole and most importantly when considered negligible, as in the current procedure, does not affect the performance of the procedure in estimating the cooling effectiveness further downstream.

c) The anisotropic turbulence model enhances the prediction of the effectiveness to the extent that the current procedure is competitive with the other methods employing the anisotropic model.

d) A turbulence model accurately accounting for the non-equilibrium nature of the jet and boundary layer interaction is expected to further enhance the prediction capability of the current and also the other numerical methods.

e) The lateral injection can be operated at much higher blowing rates to achieve a better coverage of film cooling than the streamwise injection at comparable blowing rates. The lateral injection does not have the blowing rate ceiling of M = 0.5 as in the case of streamwise injection.

f) An increase in the blowing rate increases the film cooling effectiveness on the surface when the jets are injected lateral to the mainstream.

Finally, as result of the current research, the fully-parabolic procedure is shown to be an effective tool in the field of analysis and design of film cooling systems when applied in conjunction with improved turbulence models. In addition, these findings warrant a more intense investigation of the lateral injection film cooling situation.

II. AIRFOIL SURFACE HEAT TRANSFER STUDIES

A. Turbine Blades

The influence of the turbine blade's leading edge roughness on the blade's heat (mass) transfer is investigated. The roughness, which renders the boundary layer turbulent immediately downstream of the leading edge, is simulated by placing a tripping wire on the blade's surface near it's leading edge (Sp/C=0.0375 on the pressure side and Ss/C=0.0616 on the suction side). The trip wire, 1 mm in diameter and 15 cm in length, spans the mass transfer active (naphthalene coated) height of the test blade. Thus, insuring a measurement region on the blade that is not affected by the trip's ends. A strip of sand paper (#320) is also employed to simulate the leading edge roughness. The strip covers the leading edge and terminates to Sp/C=0.0375 on the pressure side.

The influence of the boundary layer tripping on mass transfer rates (expressed as Sherwood number) is summarized in Fig. 11. On the suction side, there is a very sharp increase followed by a decrease in Sherwood number just downstream of the trip wire. This is probably due to the flow separation-reattachment created by the presence of the trip. Downstream of the flow reattachment point, the growth of the boundary layer appears to be coupled with a gradual decay of the induced turbulence to a location where the tripped and the untripped boundary layers produce the same Sherwood number. Farther downstream, however, the tripped boundary layer seems to experience an earlier and weaker (inducing less increase in mass transfer) transition than the untripped one.

On the pressure side, mass transfer does not show a rapid change behind the trip wire as it did on the suction side. It appears that the separated flow behind the trip wire and the naturally occurring separation bubble of the untripped layer merge to form an earlier, shorter, but stronger separated region. From the reattachment point downstream to the trailing edge, the tripping of the boundary layer produces only a slight increase in mass transfer. This increase will gradually diminish further downstream. The sand paper tripping of the boundary layer acts similar to the trip wire with a slight reduction in the length of the separated region and an increase in mass transfer at the reattachment point. These results, together with the response of the near endwall heat transfer to boundary layer tripping, will shortly be submitted for publication.

B. Recovery from Curvature

The purpose of this study is to document the manner in which momentum and thermal boundary layers recover from sustained concave curvature on a downstream flat-wall. Questions to be resolved include whether and where straight-wall relationships,

including turbulence models, can be applied downstream of a curved section. The study is conducted with a negligible streamwise pressure gradient in order to isolate the curvature effect. The effect of free stream turbulence is also examined.

The case with negligible free-stream turbulence intensity is now almost complete. The results of this study are reported in the attached paper by Kestoras and Simon (1991). Turbulent shear stresses have already being acquired (Fig. 12) and appear to support the conclusions of Kestoras and Simon (1991). Measurements are now being taken using the triple-wire probe built and used in previous studies in the heat transfer laboratories of the University of Minnesota. This will document for the first time, to the best of the authors' knowledge, the behavior of turbulent heat fluxes on the recovery wall downstream of a concave curvature.

The quadrant analysis (Lu and Willmarth (1973), and octant analysis (Kawaguchi et al. (1984)) will be performed on the instantaneous measurements of velocity and temperature. This is a technic that classifies the instantaneous turbulent fluctuations according to quadrants depending on the signs of instantaneous velocities and temperatures which make up the turbulent shear stress and turbulent heat flux. These quadrants are further subdivided to cold and hot motions, depending on the sign of the associated temperature fluctuations. This analysis will be helpful in determining which motions are enhanced or suppressed by the introduction and the removal of curvature, giving more insight on the associated response of mean quantities like friction coefficients and Stanton numbers.

In the very near future the high free stream turbulence generator (8% turbulence intensity) will be installed in the tunnel. Similar measurements to those taken with the negligible free stream turbulence intensity case will be performed and the two cases will be compared. The study of recovery of a boundary layer from concave curvature is to be completed by the end of the calendar year.

III. ENDWALL FLOW AND HEAT TRANSFER

A. Flow Visualization

A visualization study of the surface flow over the endwall was accomplished. This study was initiated to obtain more information about the number and the origin of the near-endwall vortices which were detected through previous mass transfer measurements. The measurements, were done on the endwall and the suction surface near the endwall (Chen and Goldstein (1988) and Goldstein and Spores (1988). The earlier results of the visualization study are compared with the results of mass transfer measurements in Jabbari

et al. (1991)) (manuscript is attached). The later results are shown in Figs. 13a and 13b. These figures show the origin and the path of some of the vortices.

B. The Two-half Blade Simulator

In the first stage of this study, a large-scale, two half-blade facility that simulates a turbine cascade flow was introduced. The simulator consists of two, large, half-blade sections, one wall simulating the pressure surface and the other wall simulating the suction surface. Two parallel endwalls constitute the third and fourth walls of the channel. Fig. 14 shows the geometry and configuration of the test blade. The advantage of this configuration is that the features of the secondary flow are large because of the relatively large test section, and the flow is easily accessible with probes. This is all done with a small delivery section compared to that of a true cascade of equal blade size. Also one can easily change the cascade geometry, such as the incidence angle, pitch, aspect ratio, and the blade shape in this simple experiment. The disadvantage is that one must verify that such a simulator replicates the features observed in a cascade. Qualification of the simulator was discussed by Chung and Simon (1990). It was shown that the cascade simulator in this investigation displayed all the essential features of a turbine cascade flow: (1) the horseshoe vortex (2) the passage vortex (3) endwall crossflow and the saddle point due to flow separation and (4) reattachment line on the suction wall, even though its geometry is very simple.

Once qualified, the facility became available for studies of the three-dimensional endwall flow with great opportunity for access and better resolution. An investigation into flow control with a fence in the endwall region was initiated first (Chung and Simon, 1991). The fence was designed to reduce some harmful effects of secondary flow on the blade surfaces It is shown to prevent the pressure-side leg of the horseshoe vortex from crossing to the suction surface and impinging on the wall. Instead, the vortex lifts and is swept downstream by the freestream as shown in Fig. 15. The vortex is weakened and decreased in size after being deflected by the fence. Such diversion of the vortex prevents it from removing the film cooling flow, allowing the flow to perform its cooling function.

Other studies will be initiated to investigate effects of various conditions which are representative of gas turbine flow. A high-turbulence generator section which is simulating the flow field from the combustor of a real gas turbine was developed. It was designed to have similar features to a combustor, such as the large scale recirculation, penetration and mixing of jets and contraction of the flow (Fig. 16). The combustor simulator, which will be located ahead of the large-scale cascade simulator, will aid in the study of the flow field and heat transfer in a cascade passage under more realistic conditions. Heat transfer visualization study is now underway with foil heaters and liquid crystal displays to observe

the mixing phenomena due to the secondary flow near the endwall and the suction wall. Before long, a new test section, which has a modern blade profile, will be fabricated. The airfoil shape will probably be similar to the C3X vane profile, as presented by Hylton, et al. (1988).

C. The New Wind Tunnel and Cascade Section

To prepare for further studies of flow and heat transfer in gas turbine engines a new cascade/wind-tunnel combination has been installed. The new tunnel is designed to produce flow velocities up to 38 m/s uniform within 0.5% over the central 90% of the cross-section of the contraction exit area (18 x 18 in.). The turbulence intensity is below 0.5%.

A literature survey was conducted to aid in the design and specification of the wind tunnel. It was concluded that a blower type tunnel with a honeycomb flow straightener, three turbulence damping screens, and a contraction ratio on the order of 6 to 9 would be sufficient to meet the goals. These parameters were sent to outside vendors and a design and cost estimate was made for in-house construction as well. Comparison of the vendor's bids, based on cost and quality of the product with the in-house estimate favored the outside vendor's proposal. Consequently, proposal of the Engineering Laboratory Design, Inc. in Lake City Minnesota, was chosen.

The purchased tunnel is a blown open jet configuration. It is equipped with a cent-axial type blower, a 30Hp induction motor, and a transistor-inverter variable-frequency speed controller. This produces flow velocities in the range of 3 - 40 m/s in the 18 x 18 inch contraction exit leading to the test section.

The walls of the tunnel are made of a laminated fiberglass reinforced plastic with a rigid foam core. The interior and exterior surfaces of the tunnel are coated with polyester gel-coat. The tunnel includes a heat exchanger to maintain uniform temperature flow and an aluminum honeycomb and three graduated damping screens to straighten the flow and reduce free stream turbulence levels. A 6.25 contraction ratio accelerates the flow between the 45x45 inch upstream section and the 18x18 inch downstream section. The wind tunnel is delivered and it is installed so that it can be operated either on a closed or an open loop configuration.

Qualification of the tunnel's performance is underway. Testing has been conducted on the uniformity of exit velocity and free stream turbulence levels are being measured. The exit flow uniformity meets our specifications, with a uniformity within 0.5% over 50% of the exit cross-section and within 1% over 90% of the cross-section. Tests also

show a slight over-shoot of the velocity near the sidewalls outside the boundary layer ranging from 2-3% depending on the mean flow velocity.

A new test section (cascade) is being designed for construction. A high visibility, acrylic test section, incorporated in the design, will facilitate flow visualization studies. The test section design also allows for easy access and quick installation of naphthalene coated, or otherwise instrumented, test blade sections. The design includes an upstream section for turbulence generation using cross-bar grids and/or jet grids, and a section for adding upstream wake generating blades ahead of the linear cascade test section, Fig. 17.

The test section will contain four blades in a central passage arrangement. The outer blades and the sidewalls will be separated by half a pitch. A flexible sidewall will be used in this region. Two tailboards will be added to the outer test blades as well. Adjustments will be made to the outer flexible wall shapes and the orientations of the two blade tailboards to produce a uniform flow within the three cascade passages.

The blades will initially have a 7.5 inch chord length, with a pitch-to-chord ratio of 0.9. All blades will be machined from aluminum. The test blade will be made from three interchangeable pieces (two spacers at 5.125 inch each and a naphthalene or pressure test blade at 7.750 inch) spanning the 18 inch test section height. The test region of the test blade can be placed in the central span of the tunnel or near the top or bottom edges for endwall measurements.

The test section is designed to allow easy access and modification. Variations of the inlet flow conditions are planned using turbulence grids, jet grids and wake-generating upstream blades. In addition, variations in the blade pitch-to-chord ratio are possible, or variations in the blade profiles can be accommodated with the open, sectional, test section design.

The new cascade test section should prove to be quite versatile for both flow visualization and mass transfer studies in countless flow conditions and test blade arrangements. The test section design is near completion and test blade manufacturing will soon be underway.

REFERENCES

Bergeles, G., Gosman, A.D., and Launder, B.E., (1975) "The Near-field Character of a Jet Discharged through a Wall at 90 deg. to a Mainstream", ASME paper 75-WA/HT-108.

Bergeles, G., Gosman, A.D., and Launder, B.E., (1976) "The Prediction of Three-Dimensional Discrete-Hole Cooling Processes. Part 1 - Laminar Flow", *ASME J. Heat Transfer*, Vol. 98c, p. 379-386.

Bergeles, G., Gosman, A.D., and Launder, B.E., (1978) "The Turbulent Jet in a Cross Stream at Low Injection Rates : A Three Dimensional Treatment", *Numerical Heat Transfer*, Vol. 1, p. 217-242.

Chen, P.H. and Goldstein, R.J., (1988) "Convective transport phenomena on a turbine blade," Proc. of the 3rd Int. Symp. on Transport Phenomena in Thermal Control, Taipei, August 14-18

Chung, J.T. and Simon, T.W., (1990) "Three-Dimensional Flow near the Blade/Endwall Junction of a Gas Turbine: Visualization in a Large-Scale Cascade Simulator," ASME Paper 90-WA/HT-4, Presented at the 1990 ASME Winter Annual Meeting, Dallas, Texas.

Chung, J.T. and Simon, T.W., (1991) "Three-Dimensional Flow near the Blade/Endwall Junction of a Gas Turbine: Application of a Boundary Layer Fence," ASME Paper 91-GT-45, Presented at the 36th International Gas Turbine and Aeroengine Congress, Orlando, Florida.

Demuren, A.O. and Rodi, W., (1983) "Three-Dimensional Calculation of Film Cooling by a Row of Jets", *Notes in Numerical Fluid Mechannics*, Vol. 7, p. 49-56.

Goldstein, R.J. and Spores, R.A., (1988) "Turbulent transport on the endwall in the region between adjacent blades," *J. of Heat Transfer*, Vol. 110(4A), p. 862-869.

Honami, S. and Fukagawa, M., (1987) "A Study of Film Cooling Behavior of Cooling Jet over a Concave Surface", *Proc. of the Joint ASME/JSME Gas Turbine Conference*, p. 1-8.

Hylton, L. D., Nirmalan, V., Sultanian, B. K. and Kaufman, R. M., (1988) "The Effects of Leading Edge and Downstream Film Cooling on Turbine Vane Heat Transfer," NASA CR-182133, 1988.

Jabbari, M.Y., Goldstein, R.J., Marston, K.C., and Eckert, E.R.G., (1991) "Three dimensional flow at the junction between a turbine blade and end-wall," To appear in the J. of Thermo-and Fluid Dynamics, Warme-und Stoffubertragung, 1992.

Kadotani, K. and Goldstein, R.J., (1977) "On the Nature of Jets Entering a Turbulent Flow - Part B: Film Cooling Performance", *Proceedings of the 1977 Tokyo Joint Gas Turbine Congress*, p. 55-59.

Kadotani, K., (1975) "Effects of Mainstream Variables on Heated and Unheated Jets Issuing from a Row of Holes", Ph.D Thesis, University of Minnesota.

Kawaguchi, Y., Matsumori, Y., and Suzuki K., (1984) "Structural Study of Momentum and Heat Transport in the Neat Wall Region of a Disturbed Turbulent Boundary Layer", *Proc. of the 9th Biennial Symposium on Turbulence*, Missouri-Rolla.

Kestoras, M.D. and Simon, T.W., (1991) "Hydrodynamic and Thermal Measurements in a Turbulent Boundary Layer Recovering from Concave Curvature," ASME Winter Annual Meeting, Atlanta, Georgia.

Launder, B.E. and Spalding, D.B., (1974) "The Numerical Computation of Turbulent Flows", *Computer Methods in Applied Mechanics and Engineering*, Vol. 3, p. 269-289.

Lu, S.S., and Willmarth, W. W., (1973) "Measurements on the Structure of the Reynolds Stress in a Turbulent Boundary Layer", *J. Fluid Mech.*, Vol. 60-3, p. 481.

Patankar, S.V. and Spalding, D.B., (1972) "A Calculation Procedure for Heat, Mass and Momentum Transfer in Three-Dimensional Parabolic Flows", *International Journal of Heat and Mass Transfer*, Vol. 15, p. 1787-1806.

Patankar, S.V., (1980), *Numerical Heat Transfer and Fluid Flow*, Hemisphere.

Patankar, S.V., Liu, C.H., and Sparrow, E.M., (1977) "Fully Developed Flow and Heat Transfer in Ducts Having Streamwise-Periodic Variations of Cross-sectional Area", *ASME J. Heat Transfer*, Vol. 99, p. 180-186.

Patankar, S.V., Rastogi, A.K., and Whitelaw, J.H., (1973) "The Effectiveness of Three-Dimensional Film-Cooling Slots - II. Predictions", *International Journal of Heat and Mass Transfer* , Vol. 16, p. 1665-1681.

Pratap, V.S. and Spalding, D.B., (1976) "Fluid Flow and Heat Transfer in Three-Dimensional Duct Flows", *International Journal of Heat and Mass Transfer* , Vol. 19, p. 1183-1188.

Raithby, G.D. and Schneider, D.B, (1979) "Numerical Solution of Problems in Incompressible Fluid Flow : Treatment of Velocity-Pressure Coupling", *Numerical Heat Transfer*, Vol. 2, p. 417-440.

Sathyamurthy, P. and Patankar, S.V., (1990) "Prediction of Film cooling with Lateral Injection", Fifth AIAA/ASME Thermophysics and Heat Transfer Conference, Seattle, Washington, June 1990, ASME HTD-vol. 138, p. 61-70.

Settari, A. and Aziz, K., (1973) "A Generalization of Additive Correction Methods for the Iterative Solution of Matrix Equations", *SIAM Journal of Numerical Analysis*, Vol. 10, p. 501-521.

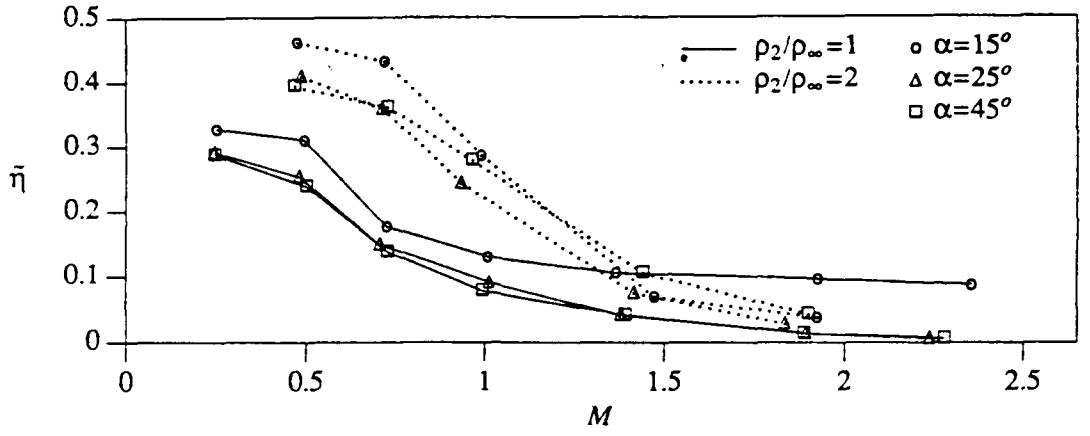

(a) x/D=4.84

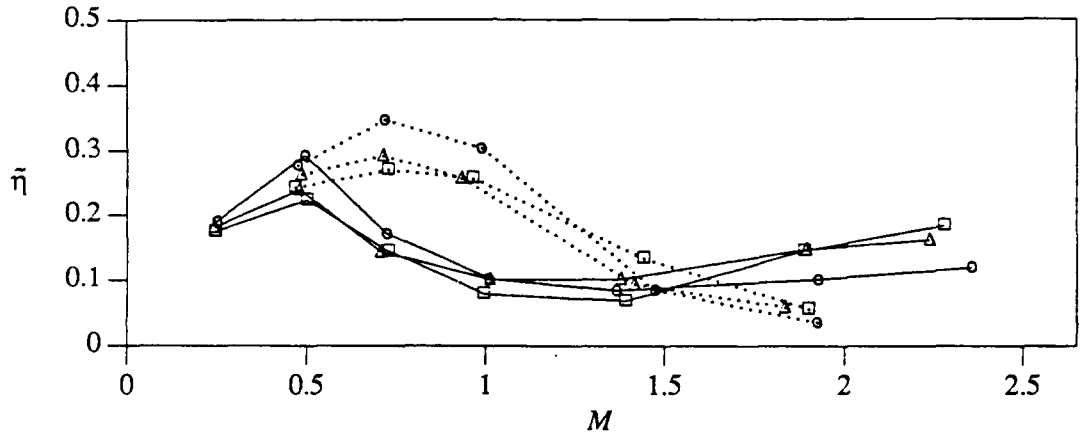

(b) x/D=17.75

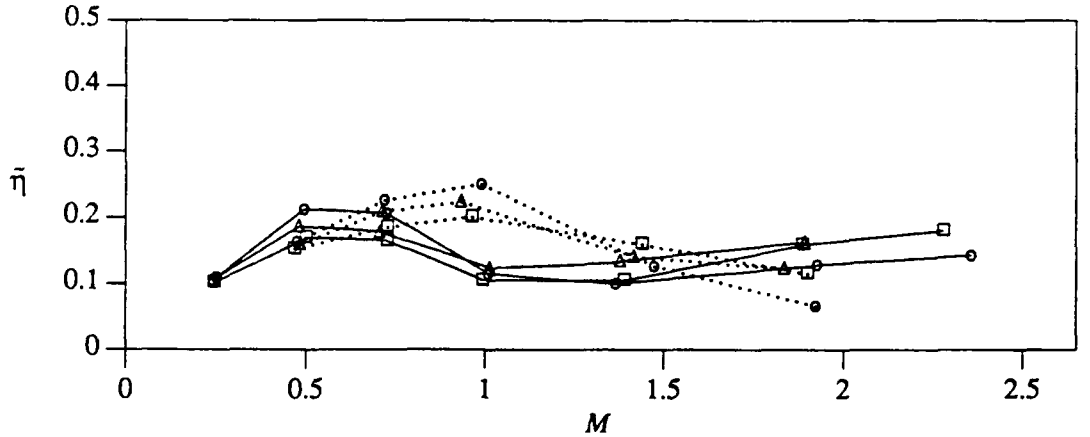

(c) x/D=45.19

Figure 1. Row-of-Holes Film Cooling on a Convex Wall: Effect of Density Ratio, Injection Angle, and Blowing Rate on Laterally-Averaged Effectiveness

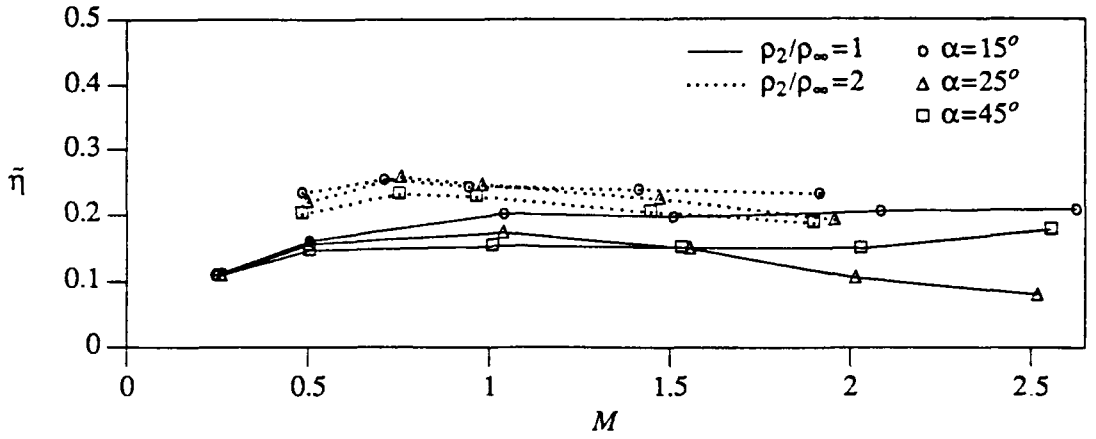

(d) $x/D=7.74$

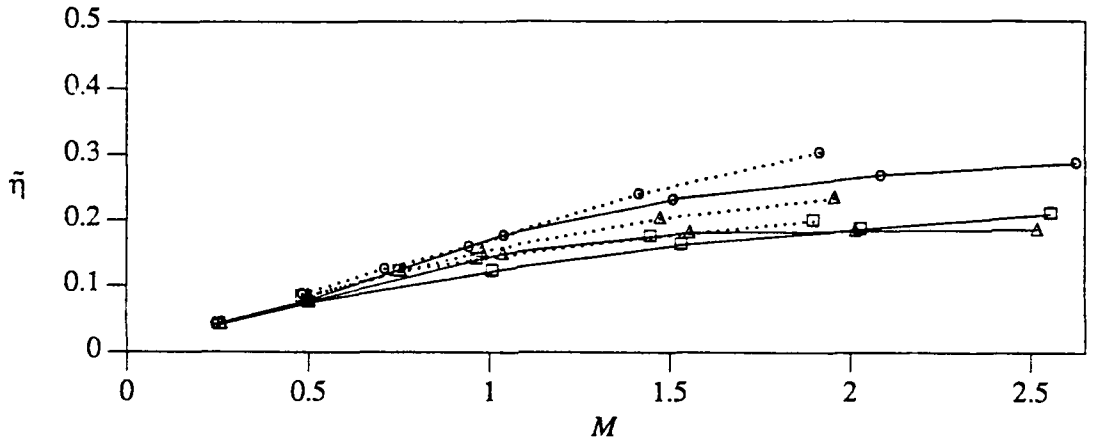

(e) $x/D=19.48$

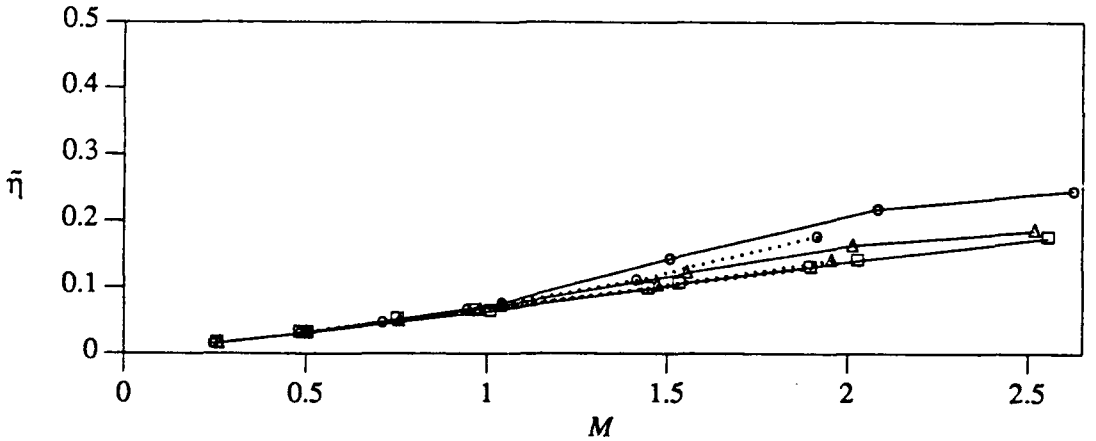

(f) $x/D=46.42$

Figure 1. Row-of-Holes Film Cooling on a Concave Wall: Effect of Density Ratio, Injection Angle, and Blowing Rate on Laterally-Averaged Effectiveness

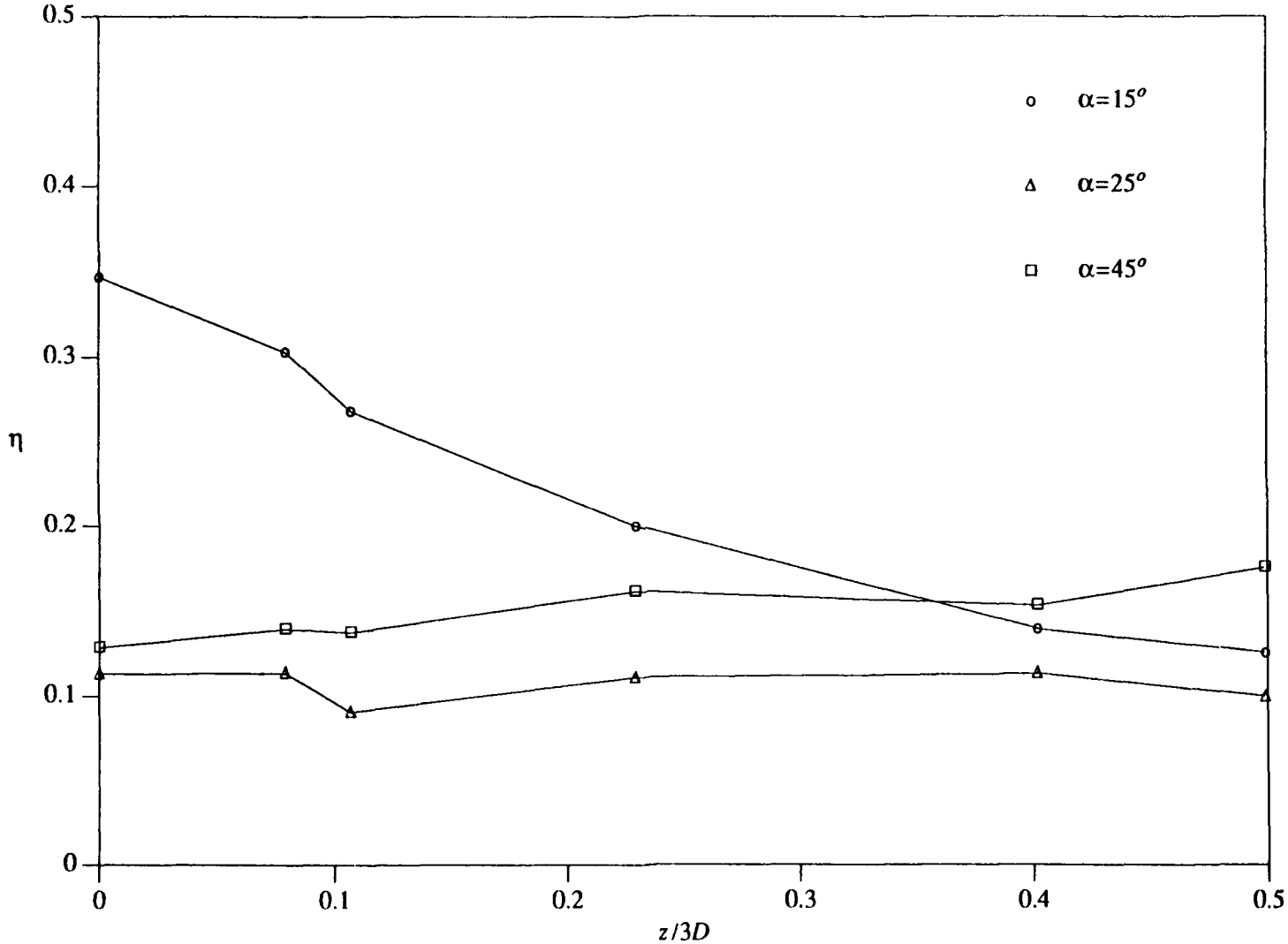

Figure 2. Lateral Profiles of Effectiveness for Row-of-Holes Film Cooling on a Concave Wall at $x/D=8, M=2.00, \rho_2/\rho_\infty=1$

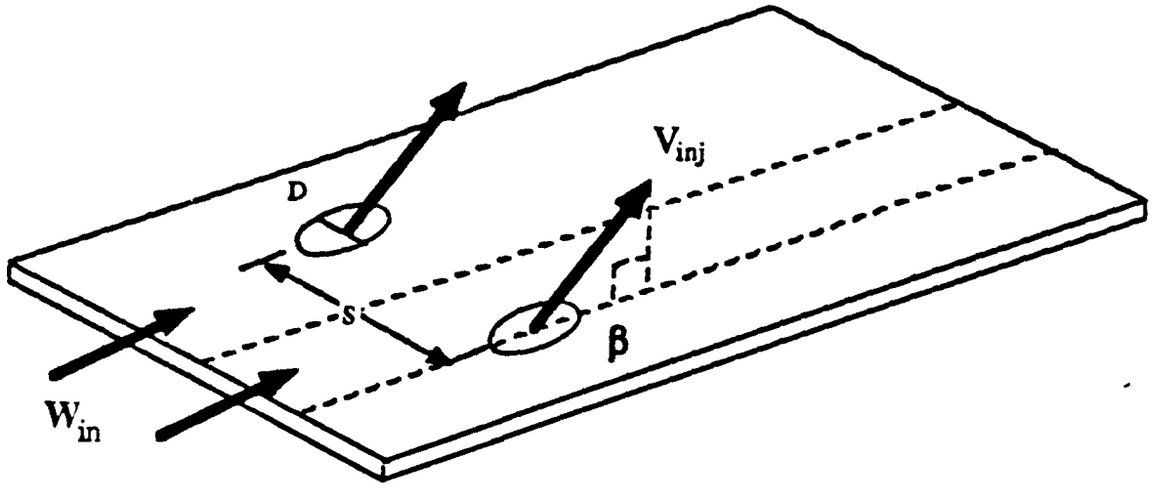

(b)

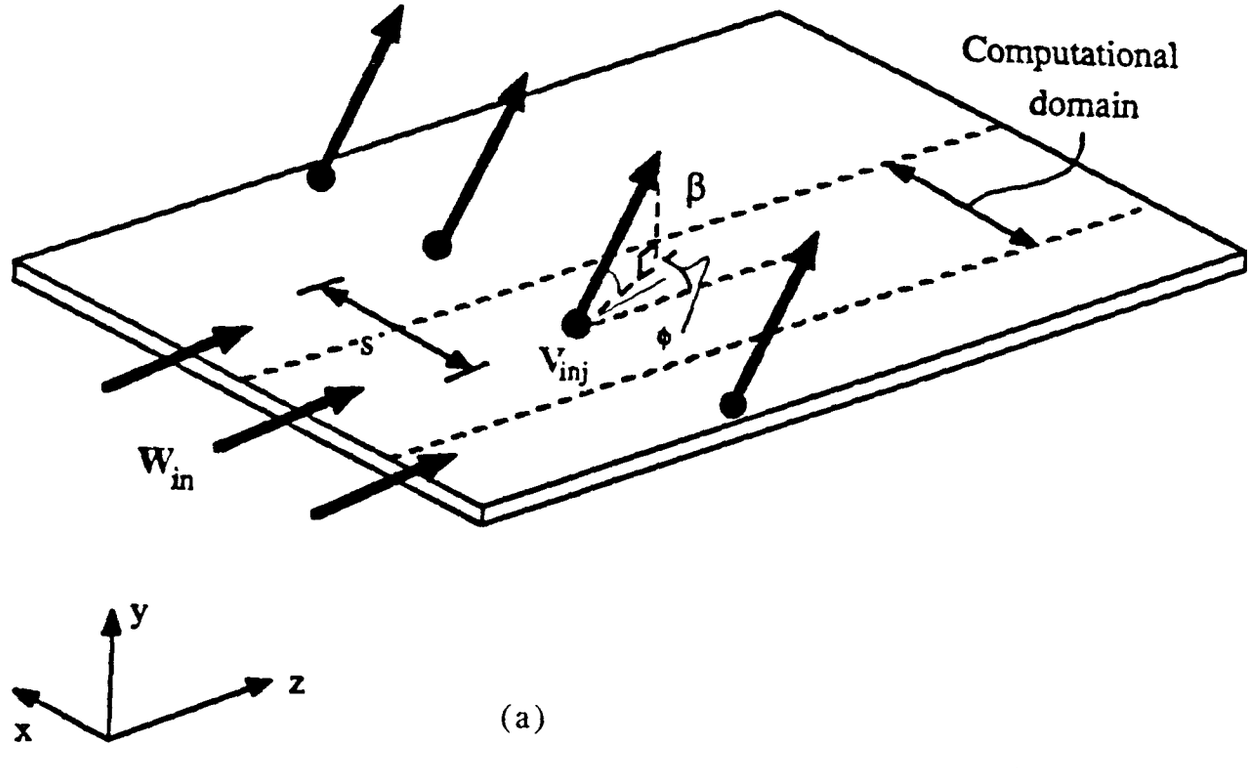

(a)

Fig. 3 Geometry of the problem.

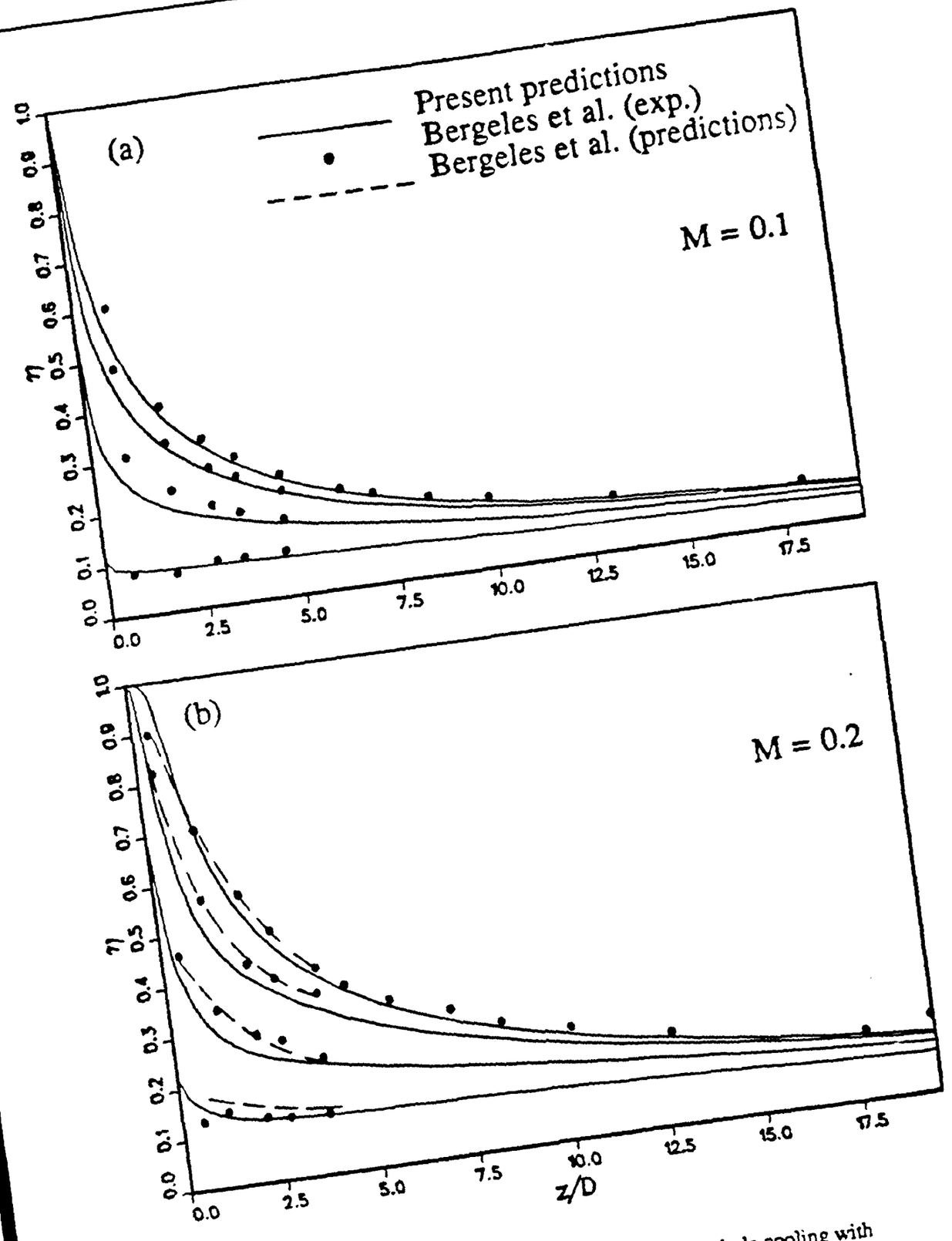

Fig. 4 Comparison of the present predictions of single hole cooling with measurements and predictions by Bergeles et al. (1975 and 1978).

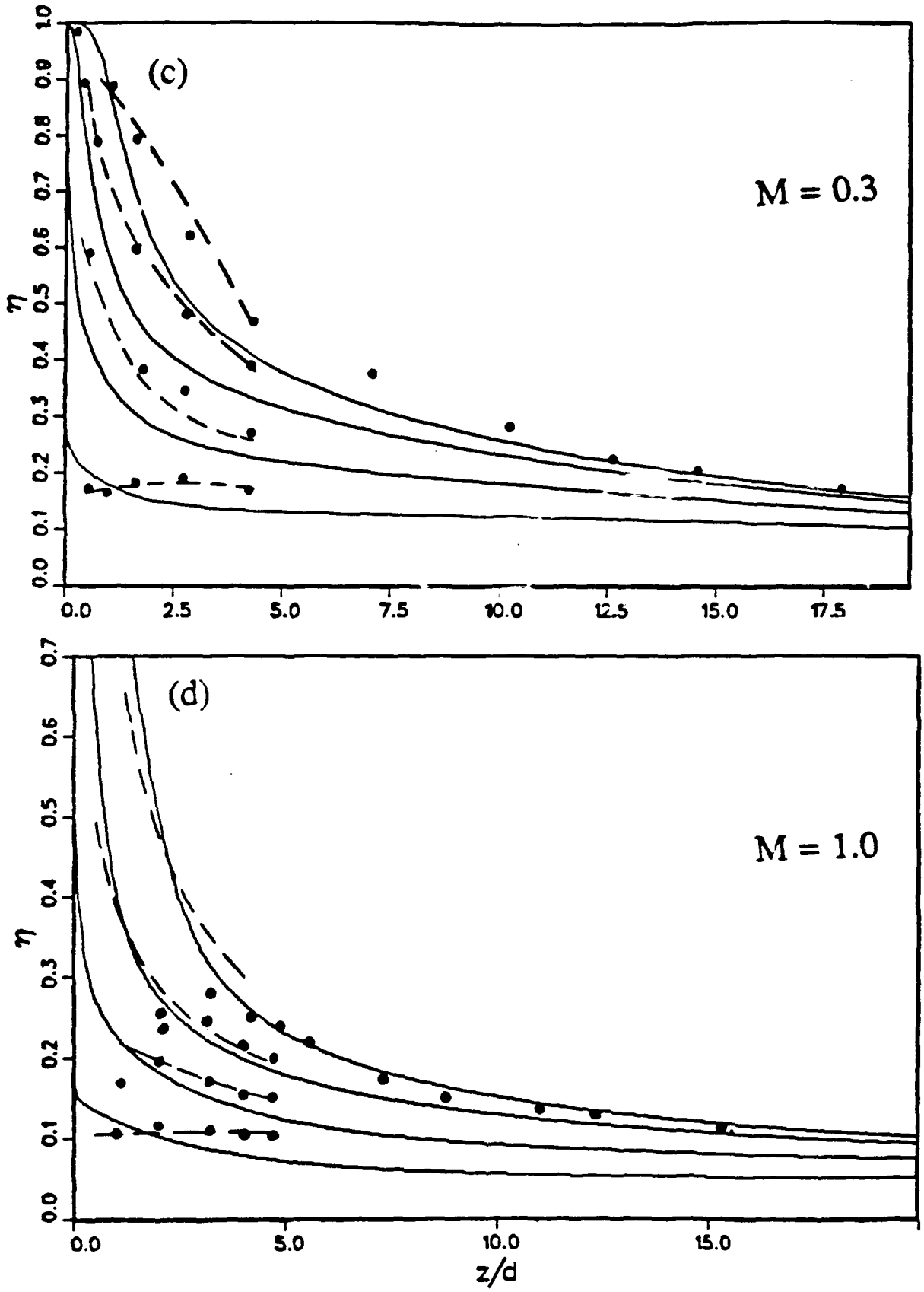

Fig. 4 Comparison of the present predictions of single hole cooling with measurements and predictions by Bergeles et al. (1975 and 1978).

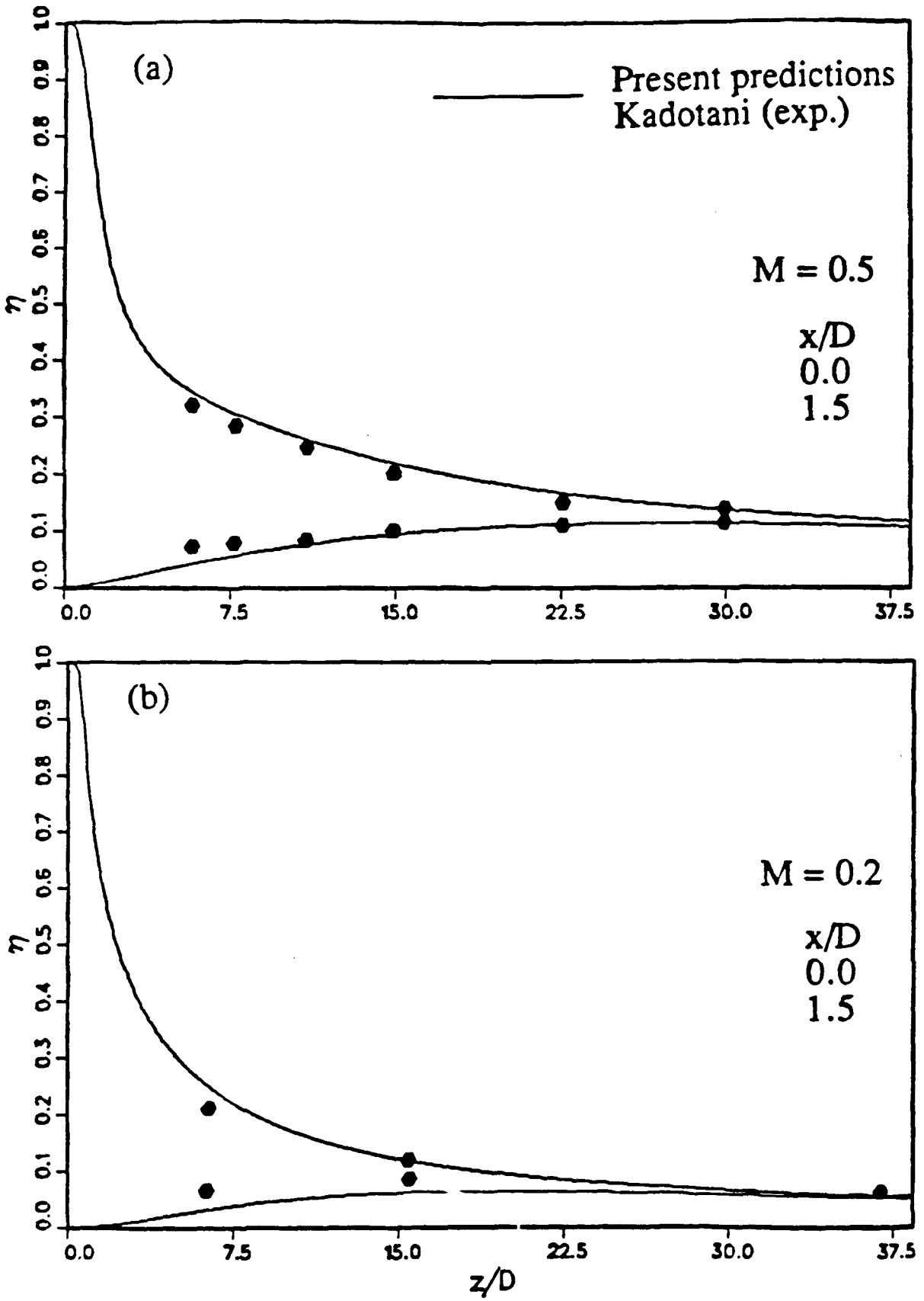

Fig. 5 Performance of the present predictions of a single row of holes cooling with measurements of Kadotani (1975).

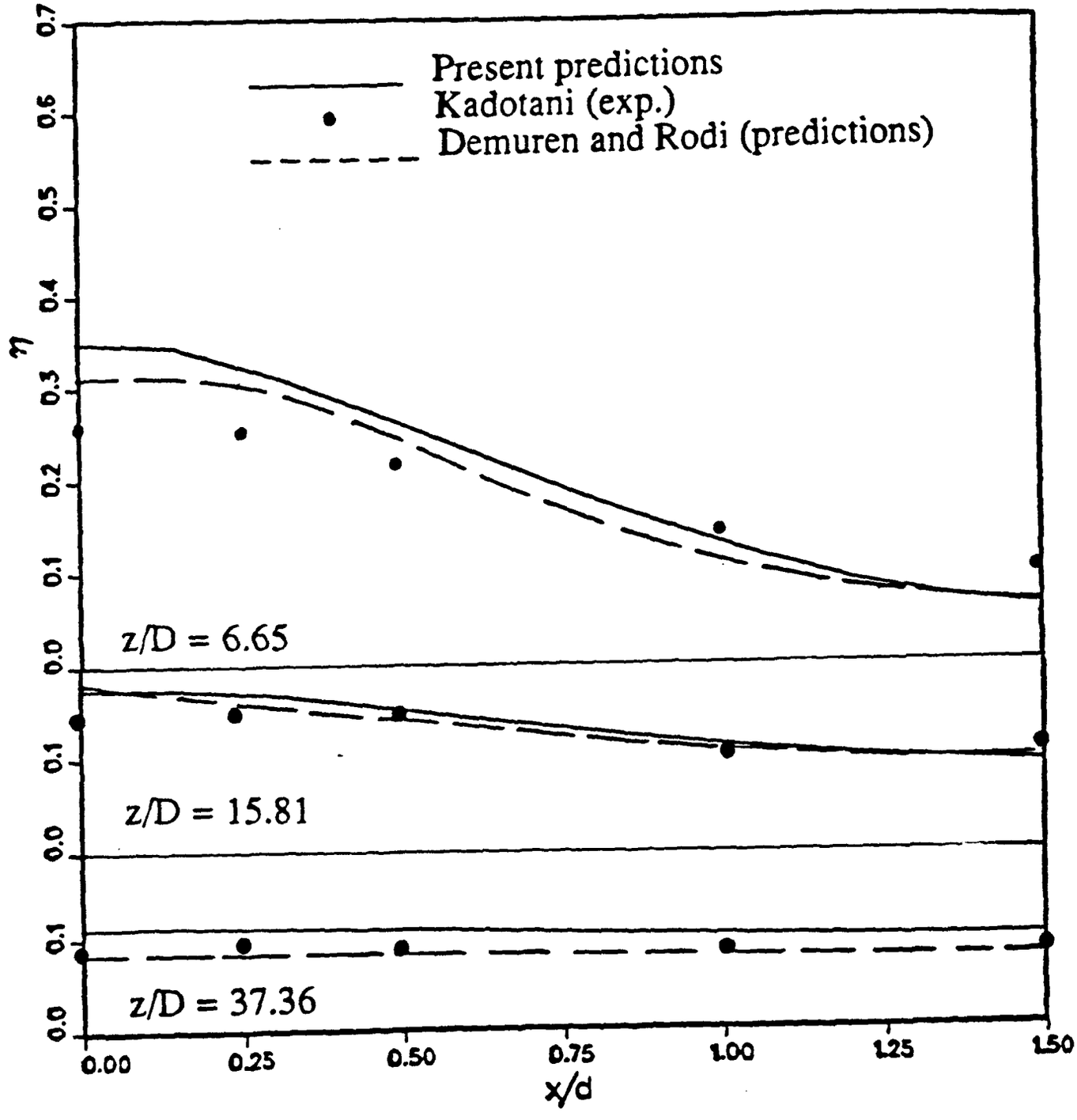

Fig. 6 Comparison of cooling effectiveness in the lateral direction at different downstream locations with measurements of Kadotani (1975) and predictions of Demuren and Rodi (1983).

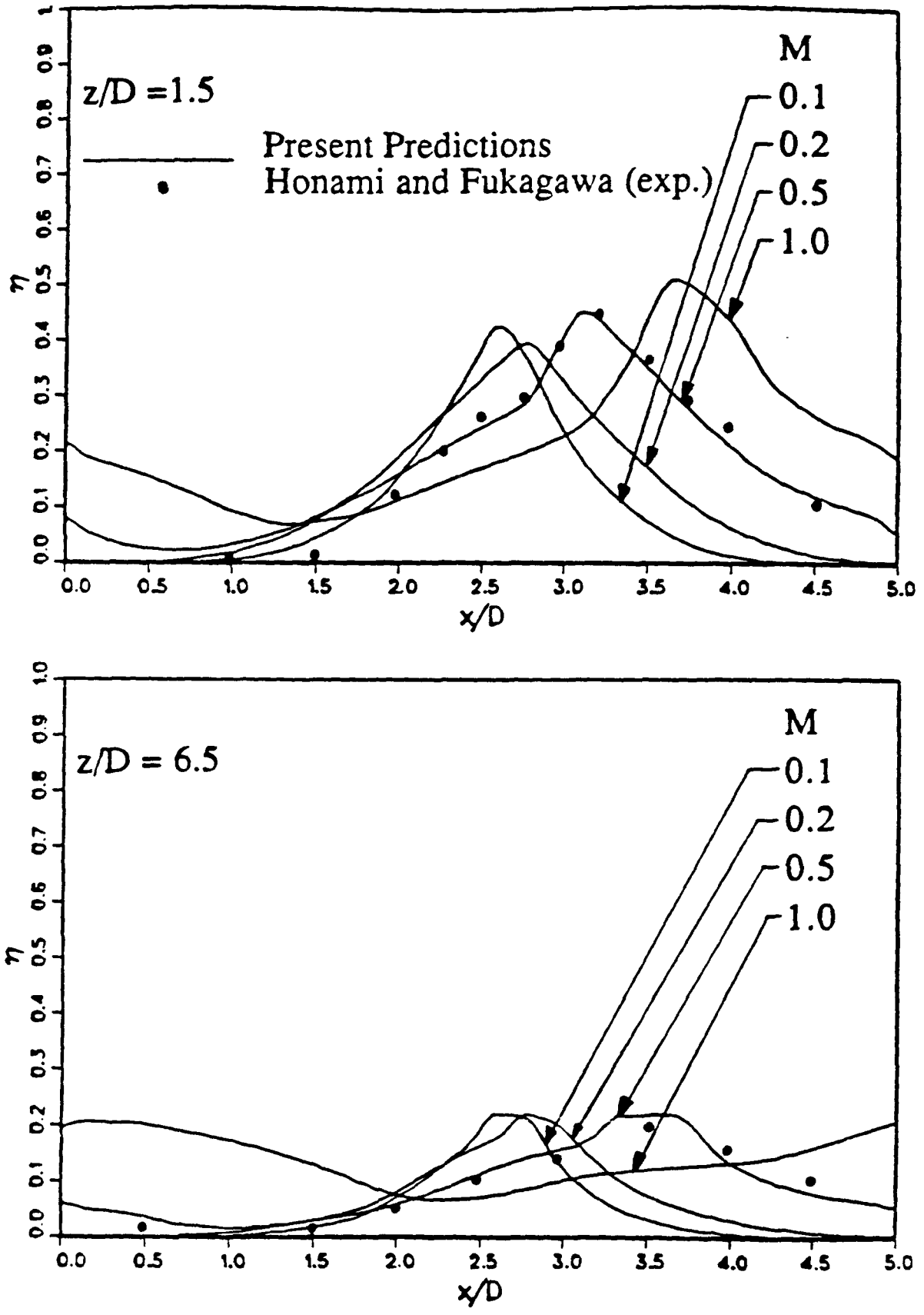

Fig. 7 Comparison of the cooling effectiveness η with the measurements at two z/D locations downstream of the injection hole.

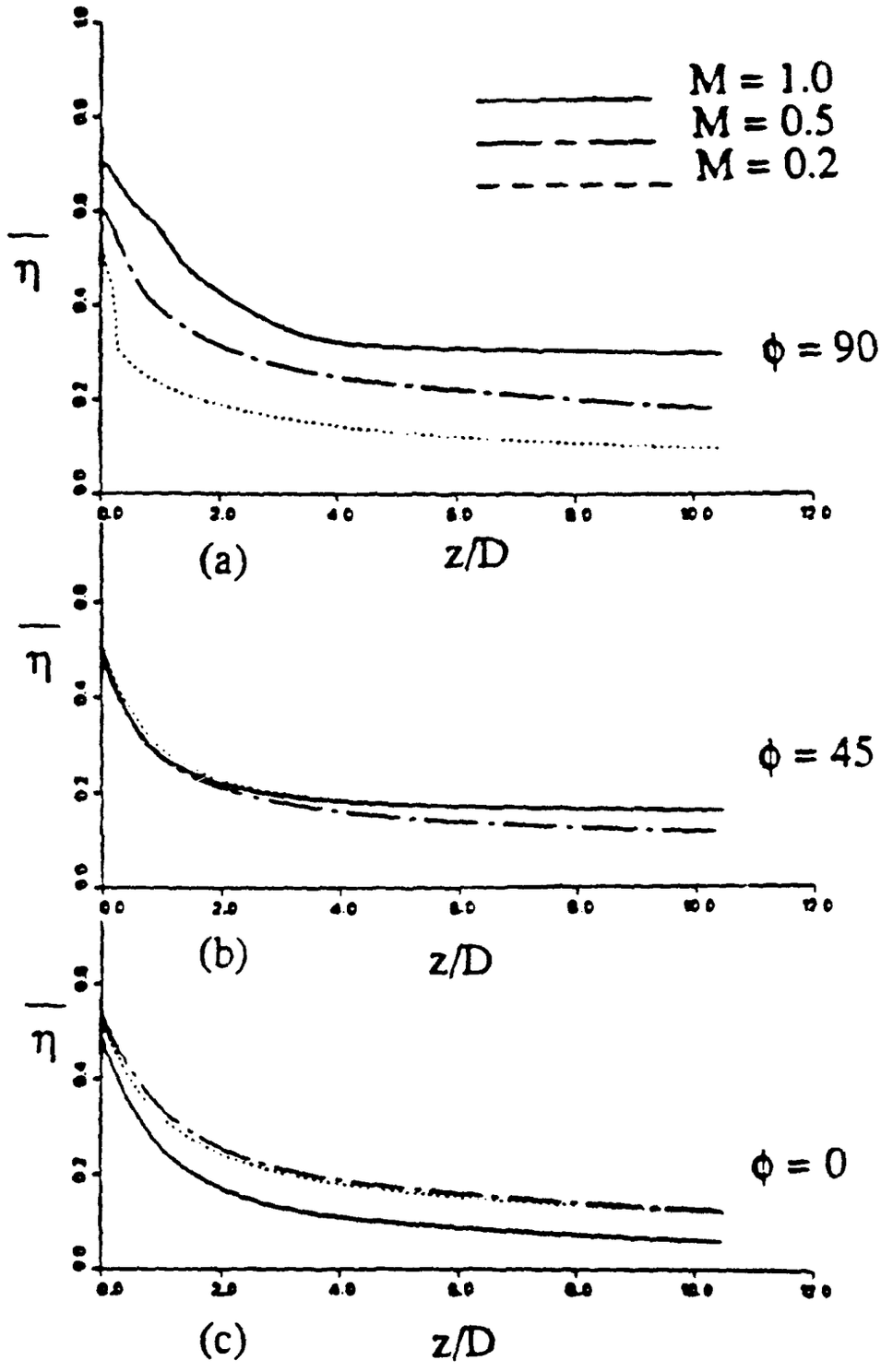

Fig. 8 Effect of blowing rate M on the laterally averaged cooling effectiveness at three lateral angles of injection for s/D = 3.

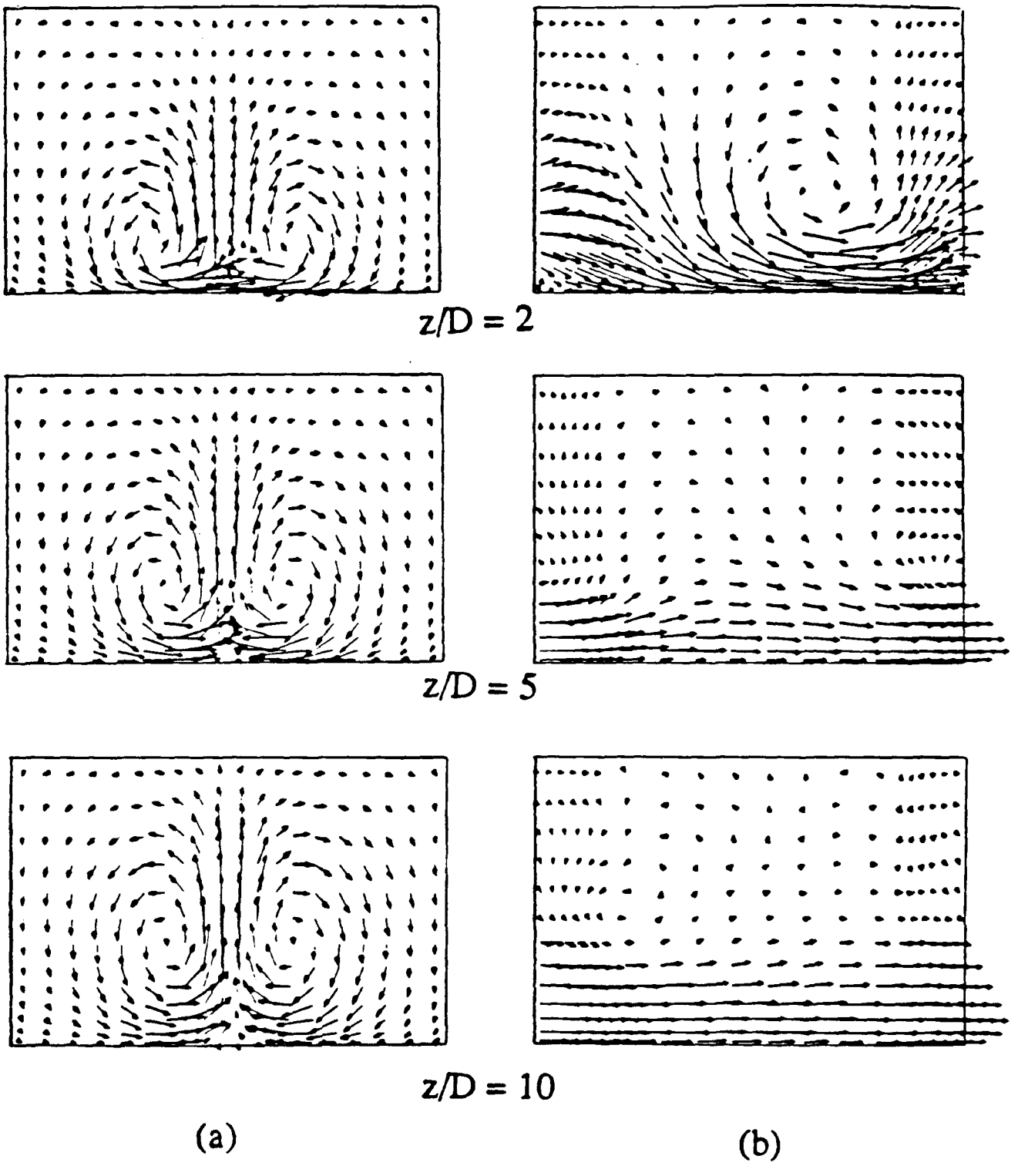

Fig. 9 Secondary flow patterns in the cross-sectional planes for M = 1 and s/D = 3
(a) streamwise injection and the resulting counter rotating vortices
(b) lateral injection and the dominant single vortex

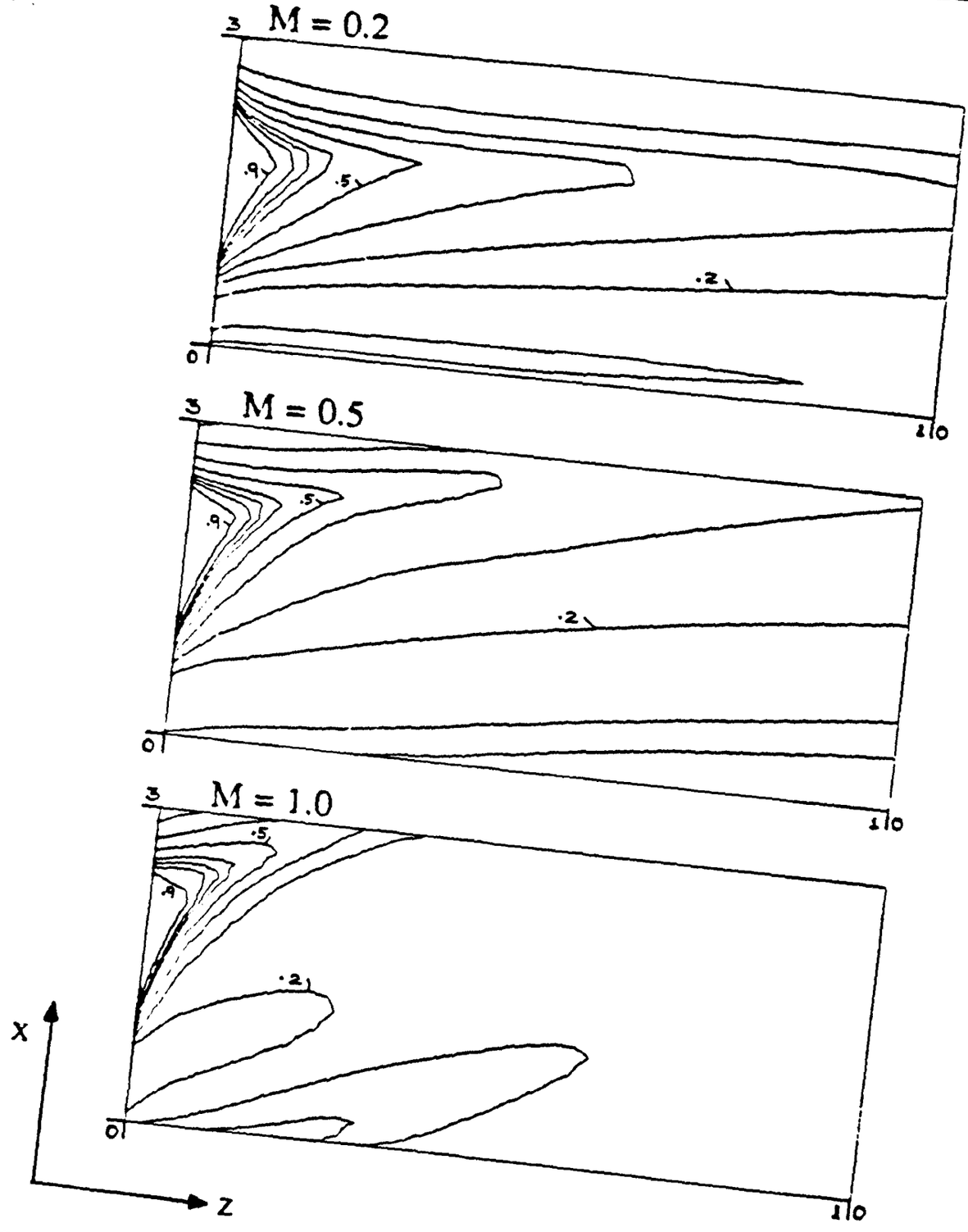

Fig. 10 Distribution of local cooling effectiveness on the plate at three blowing rates for s/D=3 and lateral injection ($\phi = 90$).

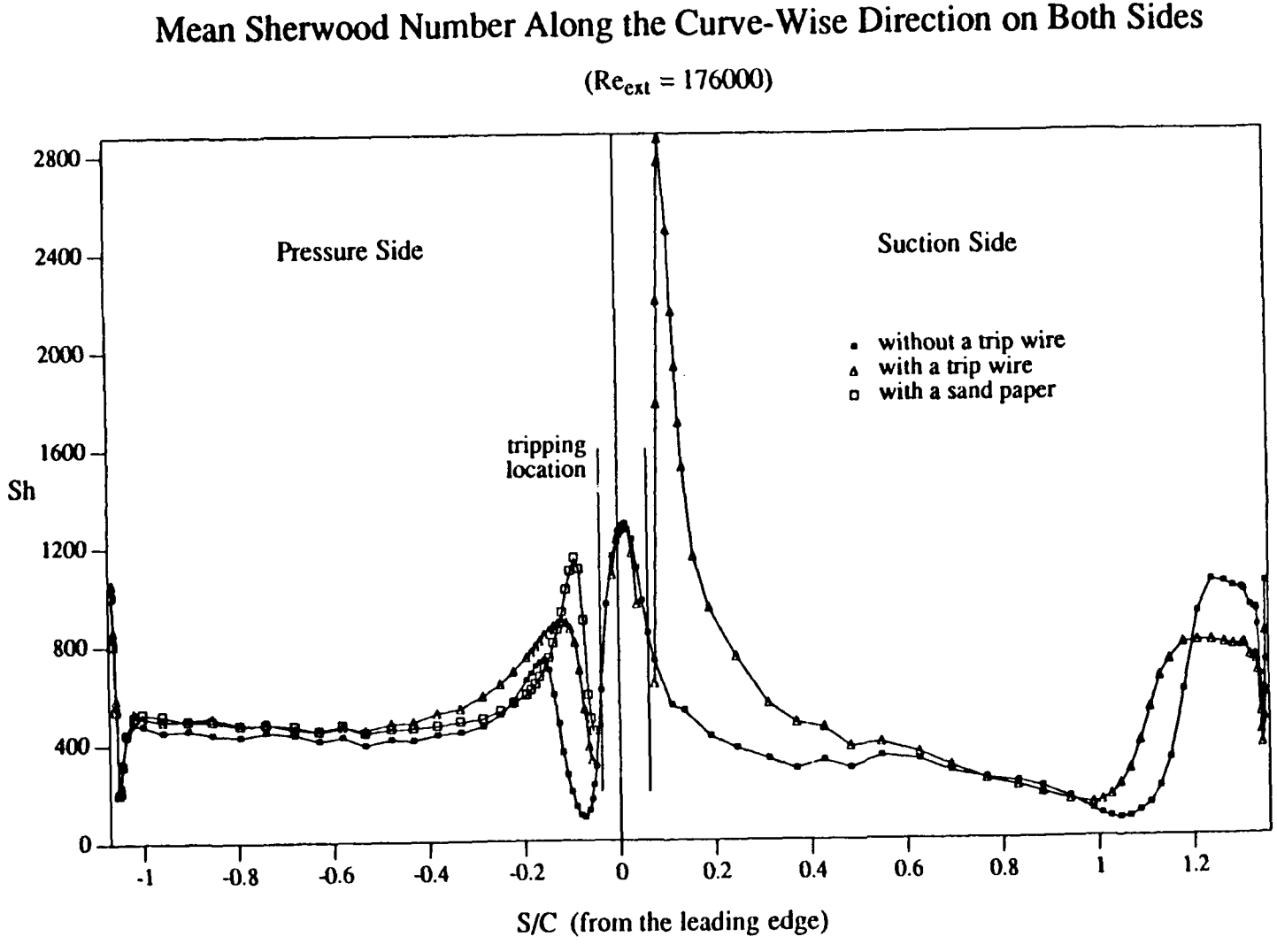

Figure 11 Effects of the boundary layer tripping on mass transfer from a turbine blade

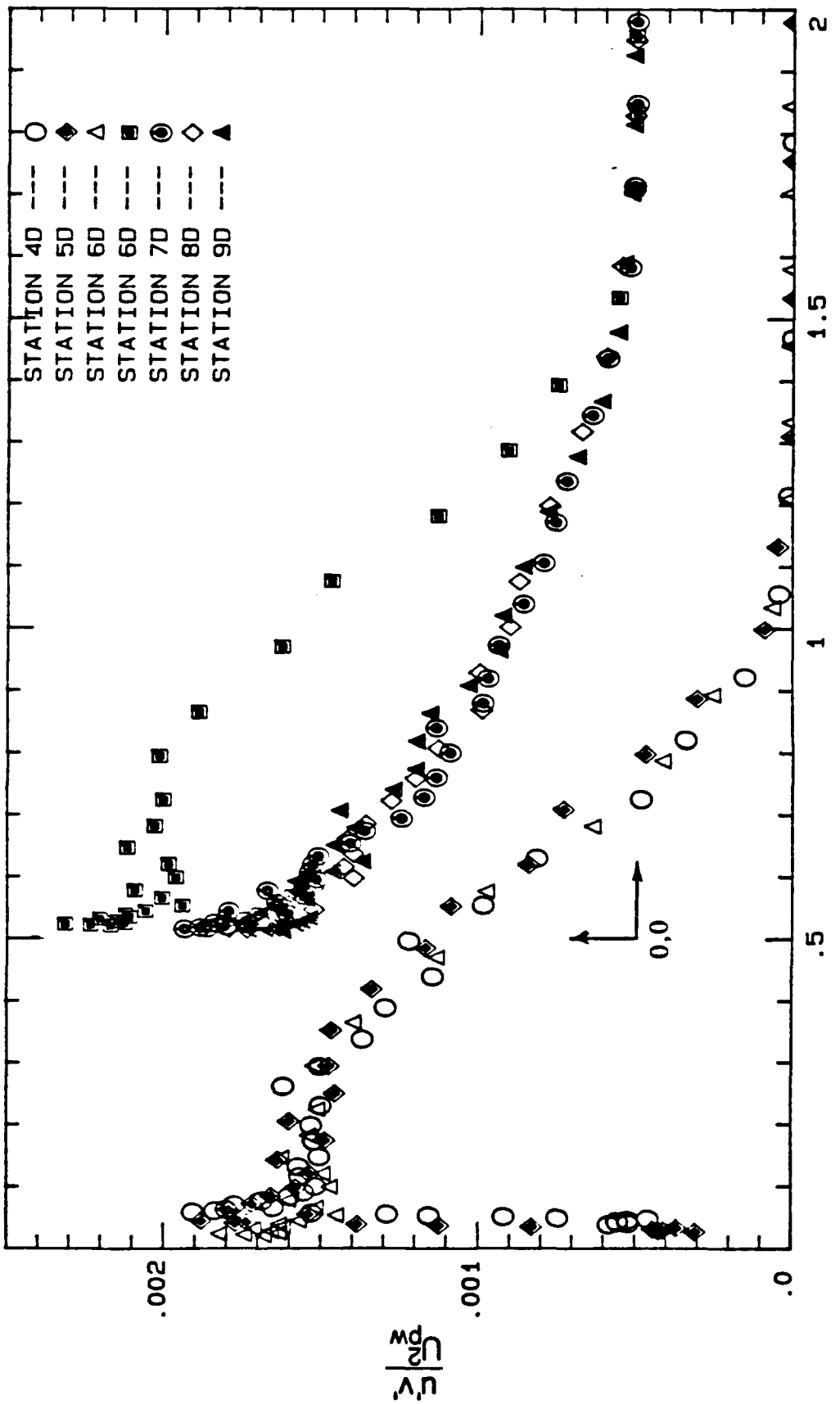

Fig. 12 Reynolds Shear Stresses at the Downwash Sites of the Göertler-like Vortices on the Concave (stations 4 and 5) and the Recovery Wall (stations 6 through 9).

Grain structure of the lamp-black visualization of the flow over the endwall suggests that the flow is consisted of several distinct regions which may end up forming various vortices in the corner of blade/endwall junction. To verify this a color visualization was developed and applied to the different regions of the flow.

Figure 13a

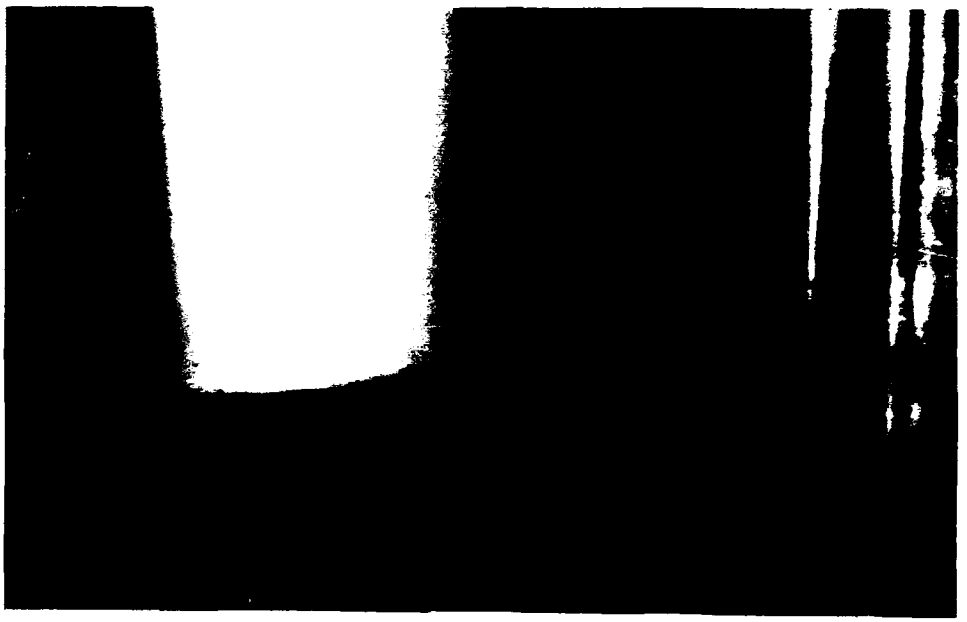

Color visualization shows that part of the near surface flow ahead of the leading edge (the flow out of the separation bubble and the suction-side leg of the horseshoe vortex, blue paint) will enter the passage, but some is pushed to converge toward the blade/endwall corner. This flow eventually is pushed to climb up over the suction surface (start of the rise of blue paint is seen but not enough paint, or momentum in the flow, to carry it further).

Flow between the dividing stream lines (red paint) will all enter the passage. The stream coming from the separation bubble of the neighboring blade forces this flow to converge to a small region along the blade/endwall junction. This flow converges from a larger span to a much smaller one , and initially has higher momentum , so it moves up the suction surface (in form of a vortex) and carries the red paint with it all the way to the trailing edge. The pressure-side leg of the horseshoe vortex of the neighboring blade breaks this vortex into two smaller ones; one continues above the endwall in touch with the suction surface, the other remains in the corner. The green and the blue paints downstream of the red are carried by the wash down flow from the pressure surface into the corner to form distinct vortices.

Figure 13b

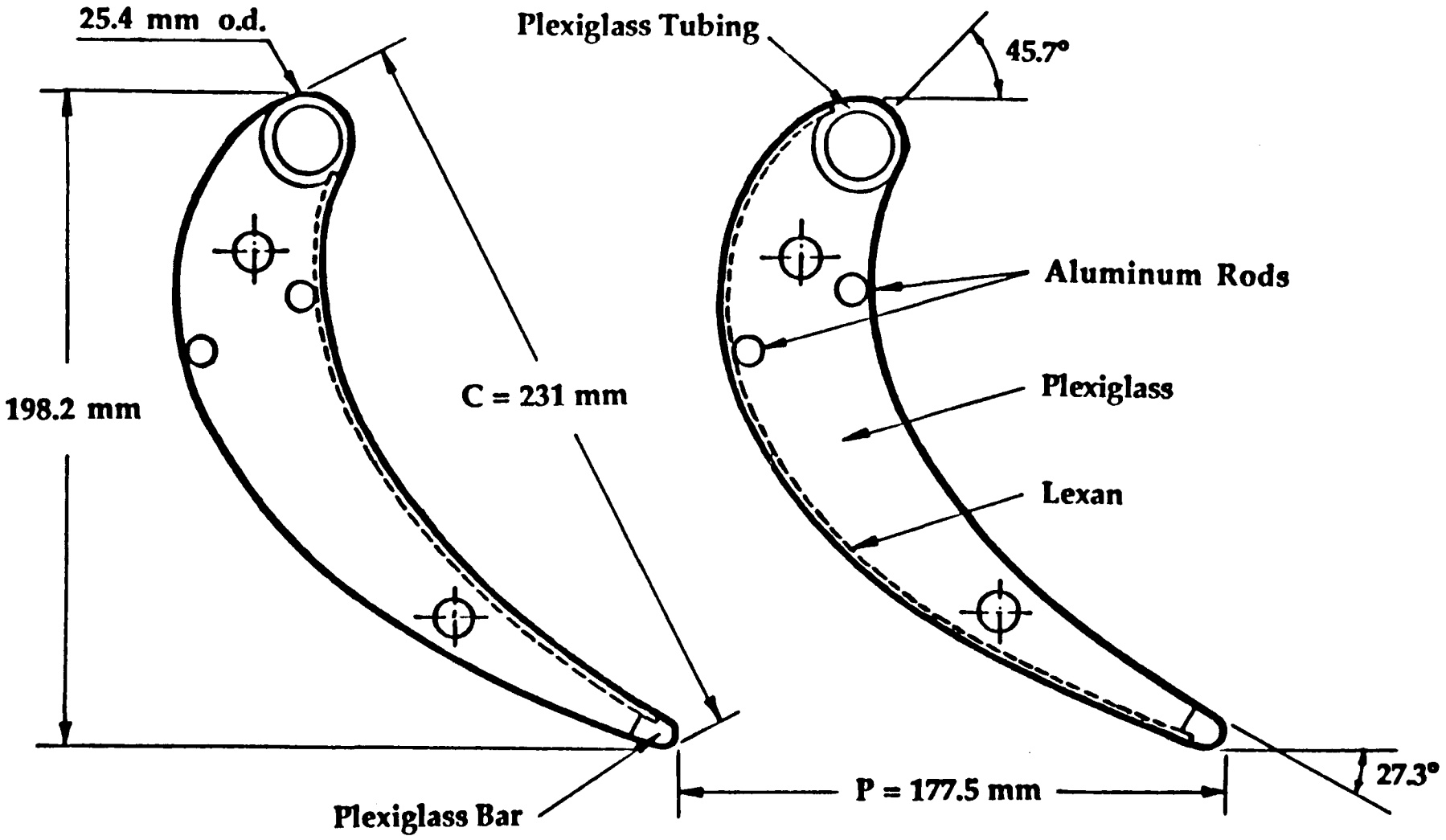

Fig. 1 4 Geometry and construction of the test section

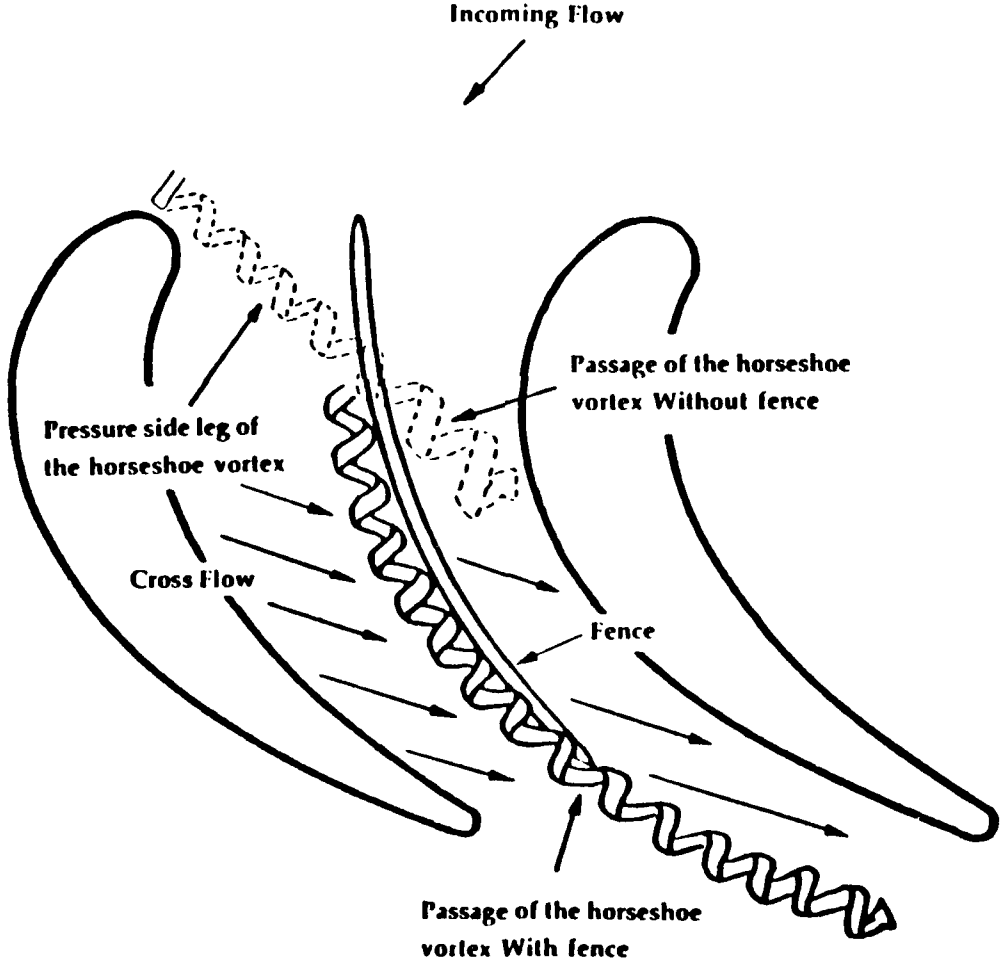

Fig. 1 5 Secondary flows in the endwall region with and without fence.

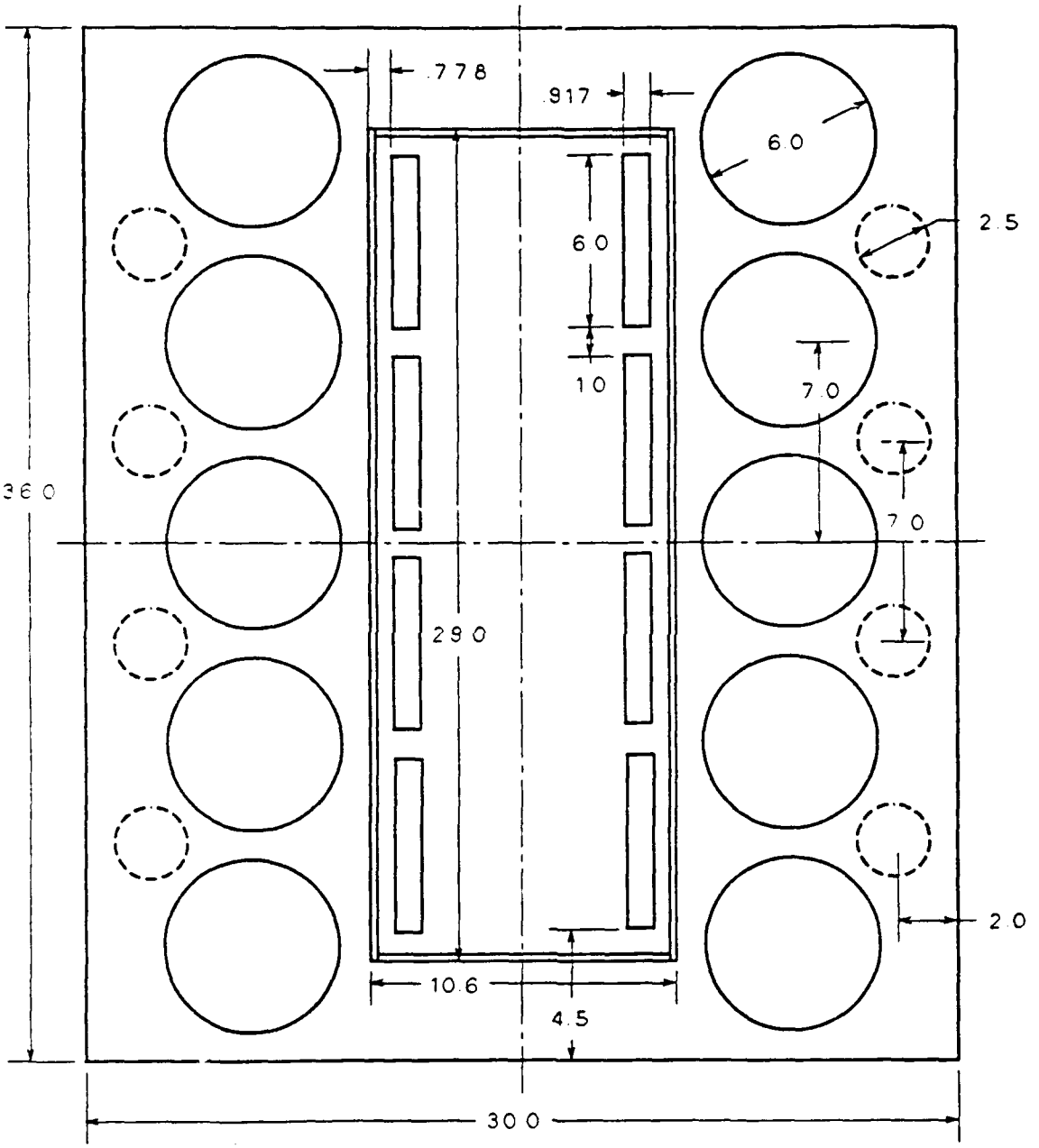

Fig. 16 Back view of turbulence generator

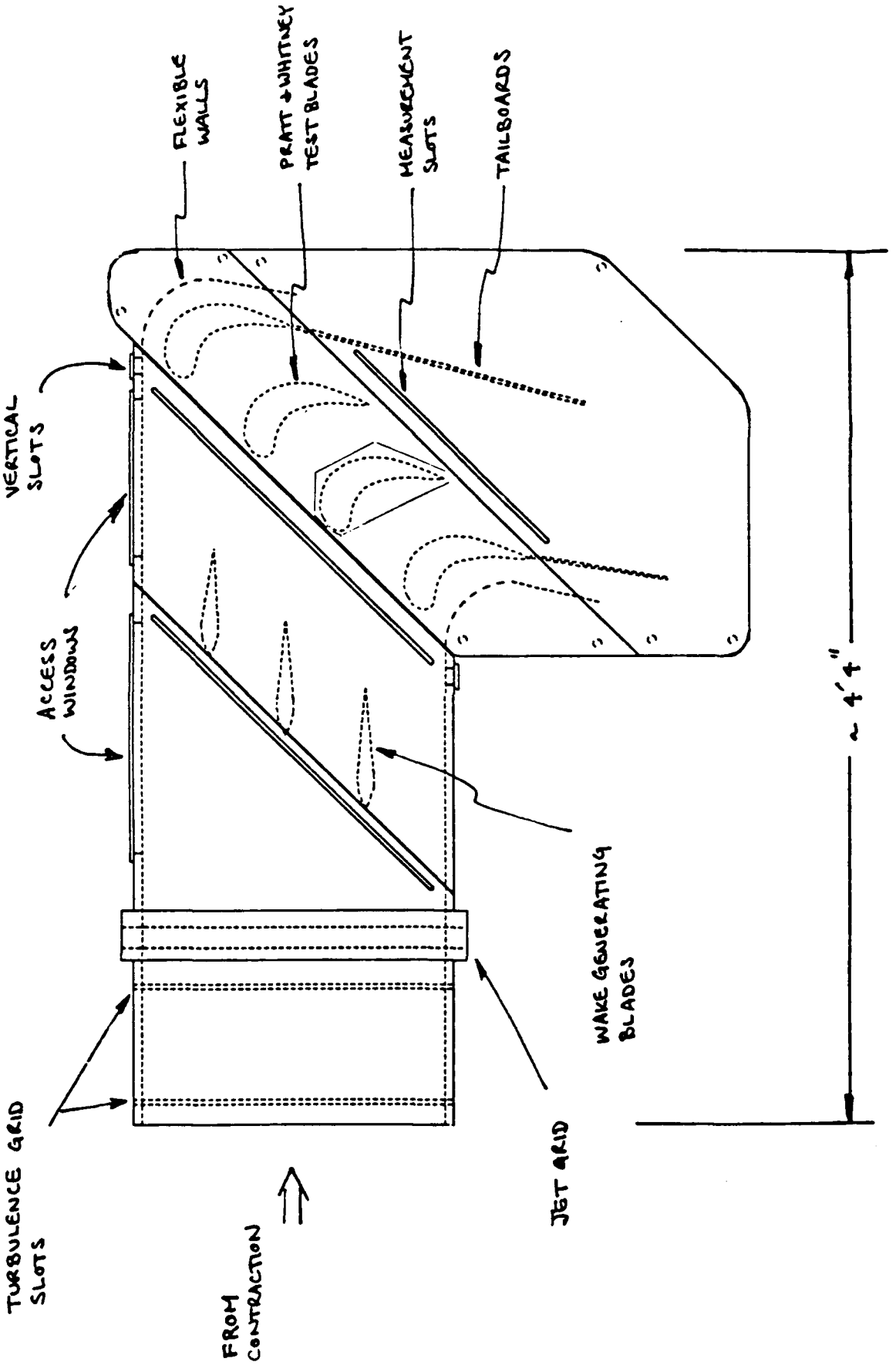

Fig.17 Sketch of the new cascade

APPENDIX I: Recent Publications on Gas Turbine Heat Transfer from the Heat Transfer Laboratory

[1] Chen, P.H. and Goldstein, R.J., (1988) "Convective transport phenomena on a turbine blade," Proc. of the 3rd Int. Symp. on Transport Phenomena in Thermal Control, Taipei, August 14-18

[2] Goldstein, R.J. and Spores, R.A., (1988) "Turbulent transport on the endwall in the region between adjacent blades," J. of Heat Transfer, Vol. 110(4A), p. 862-869.

[3] Kim, J., Simon, T.W., (1988) "Measurements of the Turbulent Transport of Heat and Momentum in Convexly Curved Boundary Layers: Effects of Curvature, Recovery and Free-Stream Turbulence," J. Turbomachinery, Vol. 110, No. 1, p. 80-87.

[4] Karni, J. and Goldstein, R.J., (1989) " Surface injection effect on mass transfer from a cylinder in crossflow: A simulation of film cooling in the leading edge region of a turbine blade"' ASME Paper 89-GT-276.

[5] Schwarz, S.G. and Goldstein, R.J., (1989) " The two-dimensional behavior of film cooling jets on concave surfaces," J. of Turbomachinery, Vol. 111, p. 124-130.

[6] Wang, T. and Simon, T.W. (1989) "Development of a Special-Purpose Test Surface Guided by Uncertainty Analysis: Introduction of a New Uncertainty Analysis Step," AIAA J. of Thermophysics and Heat Transfer, Vol. 3, No. 1, pp. 19-26, 1989.

[7] Chung, J.T. and Simon, T.W., (1990) "Three-Dimensional Flow near the Blade/Endwall Junction of a Gas Turbine: Visualization in a Large-Scale Cascade Simulator," ASME Paper # 90-WA/HT-4, Presented at the 1990 ASME Winter Annual Meeting, Dallas Texas.

[8] Goldstein, R.J., Karni J., and Zhu, Y., (1990) "Effect of boundary condition on mass transfer near the base of a cylinder in cross flow," Journal of Heat Transfer, Vol. 112, p. 501-504.

[9] Goldstein, R.J., Yoo, S.Y., and Chung, M.K., (1990) "Mass transfer from a square cylinder and its endwall in crossflow" To appear in the Int. J. of Heat and Mass Transfer Vol. 33, p 9-18.

[10] Russ, S. and Simon, T.W., (1990) "Signal Processing Using the Orthogonal Triple-wire Equations," Flowlines, the TSI quarterly magazine, Winter.

[11] Chen, P.H. and Goldstein, R.J., (1991) "Convective transport phenomena on the suction surface of a turbine blade including the influence of secondary Flows Near the Endwall," ASME Paper 91-GT-35.

[12] Chung, J.T. and Simon, T.W., (1991) "Three-Dimensional Flow near the Blade/Endwall Junction of a Gas Turbine: Application of a Boundary Layer Fence," ASME 91-GT-45, presented at the 36th International Gas Turbine and Aeroengine Congress, Orlando, Florida, 1991.

[13] Hain, R.C., Wang, H.P., Chen, P.H., and Goldstein, R.J., (1989) "A microcomputer-controlled data acquisition system for naphthalene sublimation measurement," Presented at the 11th ABCM Mech. Eng. Conf., Sao Paulo, Brazil, Dec. 1991.

[14] Kestoras, M.D. and Simon, T.W., (1991) "Hydrodynamic and Thermal Measurements in a Turbulent Boundary Layer Recovering from Concave Curvature," ASME Winter Annual Meeting.

[15] Schwarz, S.G., Goldstein, R.J., and Eckert, E.R.G., (1991), "The influence of curvature on film cooling performance," J. of Turbomachinery, Vol. 113, p. 472-478.

[16] Yoo, S.Y., Goldstein, R.J., and Chung, M.K., (1991) "Effects of Angle of Attack on Mass Transfer From a Square Cylinder and It's Base Plate," to appear in the Int. J. of Heat and Mass Transfer.

[17] Jabbari, M.Y., Goldstein, R.J., Marston, K.C., and Eckert, E.R.G., (1991) "Three dimensional flow at the junction between a turbine blade and end-wall," To appear in the J. of Thermo-and Fluid Dynamics, Warme-und Stoffubertragung, 1992.

[18] Kim, J., Simon, T.W., and Kestoras, M.D., (1990) "Fluid Mechanics and Heat Transfer Measurements in Transitional Boundary Layers Conditionally Sampled on Intermittency," submitted to the Journal of Turbomachinery.

[19] Kim, J., Simon, T.W., and Russ, S., (1990) "Free-Stream Turbulence and Concave Curvature Effects on Heated, Transitional Boundary Layers," Accepted for the Journal of Heat Transfer.

[20] Russ, S. and Simon, T.W. "Clarification and Improvements on the Rotating, Slanted, Hot-wire Technique," Accepted by Experiments in Fluids.

[21] Sathyamurthy, P. and Patankar, S.V., (1990a) "Film cooling Studies with a Three-Dimensional Parabolic Procedure", to be published.

Sathyamurthy, P. and Patankar, S.V., (1990) "Prediction of Film cooling with Lateral Injection", Fifth AIAA/ASME Thermophysics and Heat Transfer Conference, Seattle, Washington, June 1990, ASME HTD-vol. 138, p. 61-70.

APPENDIX II - Proposal and Past Progress Report.

Research on Heat Transfer Related to Development of High temperature Gas Turbines: Proposed Period 1 March 1986 - 28 February 1989.

Studies of Gas Turbine Heat Transfer, Airfoil Surface and End-Wall: Annual Progress Peport: 1 March 1985 - 28 February 1986, April 1986.

Research on Fluid Flow and Heat Transfer Relating to Development of High Temperature Gas Turbines; Proposal and Progress Report, November 1986.

Studies of Gas Turbine Heat Transfer, Airfoil Surface and End Wall: Annual Progress Report: 15 April 1986 - 15 March 1987, April 1987.

Review of Major Findings on AFOSR-sponsored Research, August 1987.

Studies of Gas Turbine Heat Transfer Airfoil Surface and End-Wall Cooling Effects Annual Progress and Forecast Report: 15 April 1987 - 1 December 1987, January 1988 (a budget for the period 3/1/88 - 2/28/89 was attached).

Studies of Gas Turbine Heat Transfer Airfoil Surface and End-Wall Cooling Effects Annual Progress Report: 1 March 1987 - 30 April 1988, March 1988.

Proposal to Air Force Office of Scientific Research--Research on Fluid Flow Relating to Development of High Temperature Gas Turbines, November 1988.

Studies of Gas Turbine Heat Transfer Airfoil Surfaces and End-Wall Cooling Effects. Final Report: 1 March 1986 - 28 February 1989, July 1989.

Research Progress and Forecast Report to The Air Force Office of Scientific Research, January 1990.

Research on Fluid Flow Relative to Development of High Temperature Gas Turbines; Progress Report, June 1990.

Fluid Mechanics and Heat Transfer Research Related to High Temperature Gas Turbines. Proposal, November 1990.

Fluid Mechanics and Heat Transfer Research Related to High Temperature Gas Turbines. Abstract, August 1991.